

UNCLASSIFIED

AD NUMBER: AD0849520

LIMITATION CHANGES

TO:

Approved for public release; distribution is unlimited.

FROM:

Distribution authorized to U.S. Gov't. agencies and their contractors; Export Control; 1 Feb 1969. Other requests shall be referred to the Office of Naval Research, Code 468, Arlington, VA 22203.

AUTHORITY

ONR ltr dtd 9 NOV 1973

AD849520

# DESIGN, CONSTRUCTION AND TESTING OF A VIBRATION ISOLATION MODULE

by  
J. J. Neville  
F. W. Boggs  
J. Thompsen

February 1969

## FINAL REPORT

Contract No. Nonr-4947(00)

STATEMENT #2 UNCLASSIFIED

This document is subject to export controls and each transmittal to foreign governments or foreign nationals may be made only with prior approval of \_\_\_\_\_

**OFFICE OF NAVAL RESEARCH  
DEPARTMENT OF THE NAVY**

WASHINGTON, D.C. 20360  
*code 468*



UNITED STATES RUBBER COMPANY  
(now UNIROYAL, Inc.)  
RESEARCH CENTER  
WAYNE, NEW JERSEY  
07470

**DESIGN, CONSTRUCTION AND TESTING OF A  
VIBRATION ISOLATION MODULE**

by

**J. J. Neville  
F. W. Boggs  
J. Thompsen**

**February 1969**

**FINAL REPORT  
Contract No. Nonr-4947(00)**

**Prepared for  
OFFICE OF NAVAL RESEARCH**

**UNITED STATES RUBBER COMPANY  
(now UNIROYAL, INC.)  
Research Center  
Wayne, New Jersey 07470**

## FOREWORD

This is the final report on the work performed by United States Rubber Company (now Uniroyal, Inc.) under Contract No. Nonr-4947(00) during the period from June 1, 1965 to June 30, 1967.

The contract was under the supervision of Director, Acoustics Programs, Naval Applications Group, Office of Naval Research, Washington, D. C. with Hugh M. Fitzpatrick as technical monitor.

The work was conducted at the Uniroyal Research Center in Wayne, New Jersey. Technical personnel who supervised and/or performed the work under the contract are as follows:

E. G. Kontos	-	Administration
D. Shichman	-	Administration
F. W. Boggs	-	Principal Investigator
J. J. Neville	-	Senior Research Engineer
J. Thompsen	-	Mechanical Engineer

## SUMMARY

A conceptual design for a Vibration Isolation Module (VIM) which can be incorporated into a cable-towed instrumentation body is described and analyzed.

The VIM was designed to attenuate significantly vibrations over a frequency range from  $10^{-1}$  cps to higher frequencies likely to be encountered. The design principles of the VIM are independent of the particular towed body, therefore only construction details would have to be changed to use the same principles in conjunction with other towed bodies.

A prototype VIM was constructed and tested. It involved the use of a multiple piston arrangement in which the stagnation pressure at the fore end of the VIM was converted to a force which matched the drag of the towed body. In this way it was possible to preserve a low modulus while avoiding a high elongation, since the main towing effort was balanced in such a way that the damping mechanism carried only the fluctuation and not the active force.

During tests, the VIM did not attenuate in the frequency range for which it was designed (below 5 cycles per second).

The primary cause of the failure to meet design requirements was the high level of the frictional forces. Detrimental hydrodynamic forces were also encountered. These are attributed mostly to water flow through the many orifices and channels.

During the course of this work several alternative designs were considered. These efforts are described in the Appendix.

Faint, illegible text, possibly bleed-through from the reverse side of the page.

## TABLE OF CONTENTS

	<u>Page</u>
SUMMARY . . . . .	111
1.0 INTRODUCTION . . . . .	1
2.0 DESIGN REQUIREMENTS . . . . .	3
3.0 THEORETICAL ANALYSIS . . . . .	8
3.1 STABILITY ANALYSIS OF A CONVENTIONAL VIM . . . . .	8
3.2 PRINCIPLE OF ACTION OF PROPOSED VIM . . . . .	10
3.3 DISCUSSION OF VIBRATION TRANSFER FUNCTION OF VIM . . . . .	14
3.4 EFFECT OF BLADDER ON VIM PERFORMANCE . . . . .	20
4.0 DESIGN AND CONSTRUCTION OF MODEL . . . . .	25
4.1 DESIGN ANALYSIS . . . . .	25
4.2 CHOICE OF MATERIALS . . . . .	27
4.3 CONSTRUCTION OF MODEL . . . . .	27
5.0 VIBRATION TESTS . . . . .	29
5.1 TEST APPARATUS . . . . .	29
5.2 TEST RESULTS . . . . .	29
6.0 DISCUSSION . . . . .	38
APPENDIX - ALTERNATIVE VIM DESIGNS . . . . .	41
DISTRIBUTION LIST . . . . .	51

LIST OF FIGURES

<u>Figure</u>		<u>Page</u>
1.	Oscillating loads on towed cable . . . . .	1
2.	Stagnation pressure and drag vs. tow velocity for cylinder 300 ft. long and 3 in. in diameter . . . . .	5
3.	Prototype VIM in mid-stroke attitude . . . . .	7
4.	Schematic representation of VIM . . . . .	11
5.	Transmissibility ratio vs. frequency . . . . .	21
6.	Conceptual design of VIM . . . . .	26
7.	Test apparatus . . . . .	30
8.	Force-generating capacity of VIM . . . . .	32
9.	Four sealing rings, evaluated for low friction . . . . .	33
10.	Attenuating capacity of VIM . . . . .	35
11.	Output amplitude of VIM under no load as a function of frequency . . . . .	37
12.	Comparison of theoretical and experimental results . . . . .	39



## LIST OF SYMBOLS

a	a real number
$a_z$	frictional term in $Z_3$
A	area of the piston ( $\text{ft}^2$ )
b	a real number
$b_z$	frictional term in $Z_3$
B	a constant
c	a real number
C	a constant
$C_D$	drag coefficient of tow body ( $3 \times 10^{-3}$ )
$C_1, C_2$	normal dashpot constants of soft and hard springs respectively $\left( \frac{\text{lb}_f \text{sec}}{\text{ft}} \right)$
d	a real number
$D_c$	cable diameter (ft)
D	differentiation with respect to time
e	elongation of soft spring in VIM (ft)
f	frequency (cps)
$f_c$	frequency cutoff (cps)
$f(l)$	a function of $l$
F	drag force ( $\text{lb}_f$ )
$g(e)$	some function of e
$h(t)$	some function of t
$\bar{h}$	Fourier transform of h
i	$\sqrt{-1}$
k	reciprocal spring constant of bladder associated with V $(\text{ft}^5/\text{lb}_f)$

$K$	spring constant of conventional VIM ( $\text{lb}_f/\text{ft}$ )
$K_1', K_2'$	normal spring constants of soft and hard springs respectively ( $\text{lb}_f/\text{ft}$ )
$K_1, K_2$	complex spring constants of soft and hard springs respectively $K_1 = K_1' + i\omega c_1$ , $K_2 = K_2' + i\omega c_1$
$l$	total length of casing (ft)
$l_0$	length of VIM (ft)
$L_0$	length of towed body (ft)
$M_E$	effective mass of the VIM and towed body ( $\text{lb}_m$ )
$M_1$	mass of piston in VIM ( $\text{lb}_m$ )
$M_2$	effective mass of VIM ( $\text{lb}_m$ )
$M_3$	effective mass of towed body ( $\text{lb}_m$ )
$P_0$	the stagnation pressure (psi)
$P_1$	the ambient pressure (psi)
$P_2$	stagnation pressure acting on the piston in the VIM
$P_D$	the dynamic pressure (psi)
$q$	dynamic pressure (psi) $q = 1/2 \rho U_\infty^2$
$Q_j$	generalized force in Lagrange's equation
$R$	radius of casing (ft)
$S$	Strouhal Number
$S_w$	wetted area of tow body ( $\text{ft}^2$ )
$t$	time (sec)
$T$	kinetic energy function
$u$	fluctuation velocity (ft/sec)
$U_1$	instantaneous velocity of the piston in the VIM (ft/sec)
	$U_1 = U_\infty + u$

$U_2$	the instantaneous velocity of the VIM (ft/sec)
$U_\infty$	velocity of tow (ft/sec or knots)
$\bar{V}$	mean rate of flow between scoop and cylinder (ft <sup>3</sup> /sec)
$V$	potential energy function
$V_0$	equilibrium volume in VIM in which $P_2$ acts
$V_1$	instantaneous volume in VIM in which $P_2$ acts
$ W(i\omega) $	transmissibility function
$x_{10}, x_{20}, x_{30}$	equilibrium positions of VIM - towed body system
$x_j$	cartesian coordinate ( $j = 1, 2, 3$ )
$\bar{x}_j$	Fourier transform of $x_j$
$Z_1, Z_2, Z_3$	linear operators of $D$
$\alpha$	stability exponent
$\gamma$	added mass coefficient
$\delta_{ij}$	Kronecker delta
$\dot{\eta}$	dimensionless velocity $\dot{\eta} = \frac{\dot{u}}{U_\infty}$
$\dot{\theta}$	dimensionless velocity $\dot{\theta} = \frac{\dot{u}}{U_\infty} - \frac{\dot{e}}{U_\infty}$
$\xi$	small elongation of casing
$\tau$	relaxation time
$\rho$	density of water (2 lb <sub>f</sub> sec <sup>2</sup> /ft <sup>4</sup> )
$\psi$	an angle
$\omega$	angular frequency $\omega = 2\pi f$

**BLANK PAGE**

## 1.0 INTRODUCTION

The performance of a towed instrument may be adversely affected by vibrations which are transmitted to it from the towing cable. These vibrations are from several sources, such as motion of the towing craft, turbulence of the cable boundary layer, and unstable flow about the cable (vortex shedding). Performance of such a system may be greatly enhanced by inserting between the towing cable and the towed body a Vibration Isolation Module (VIM) whose function is to damp out vibrations over a range of frequency and amplitude. The present contract was undertaken to improve the performance of the VIM and was carried out in three phases: theoretical study, design and construction of a prototype, and performance testing.

In towing systems there is a combination of steady and time-varying forces applied to the cable by the attachments to its ends and fluid reactions along its length. The steady forces are due to the end loads, weight and fluid drag along the cable. Time-varying loads are caused by motion of the towing craft, unstable flow (vortex shedding) about the cable, turbulence of the cable boundary layer and the turbulent wake of the towing craft<sup>1</sup>. (See Figure 1)

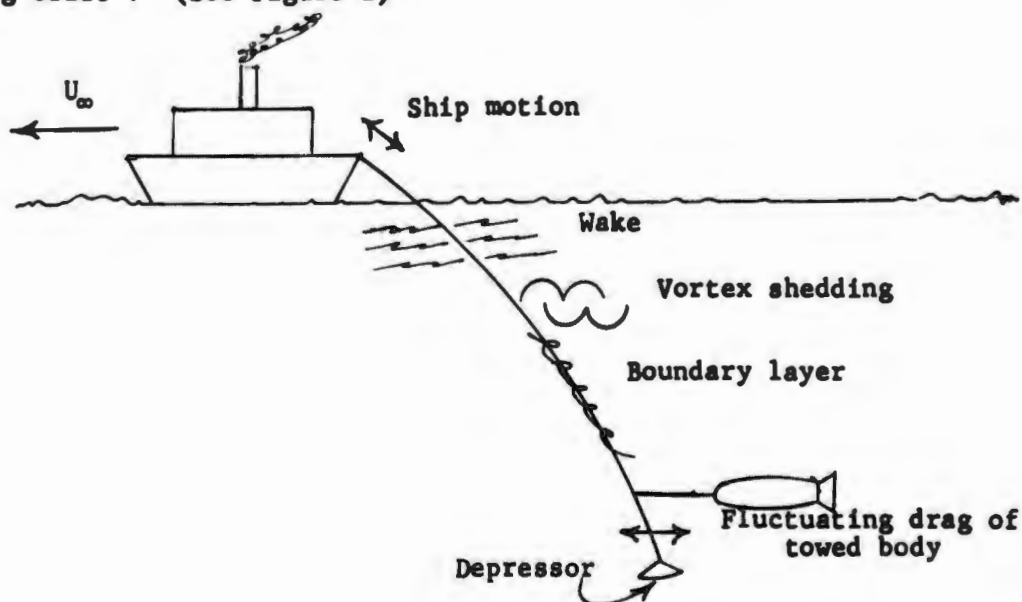


Figure 1. Oscillating Loads on Towed Cable

(1). Lyon, R.H., "The Transmission of Vibrations by Towed Cables," Final Report, Navy Contract No. Nonr-3468(00). May 28, 1962.

These time-varying loads can result in vibrations in the point of attachment of the cable and the towed body.

A conceptual design of a VIM employing a soft spring to damp out low frequency disturbances and a hard spring to damp out high frequency disturbances is described in this report. This design, which balances the high preloading (due to the drag force) on the soft spring by an equal and opposite force proportional to the dynamic pressure, is potentially operational over the entire velocity range of interest, since the drag force and dynamic pressure are both proportional to the velocity squared.

## 2.0 DESIGN REQUIREMENTS

Lyon<sup>1</sup> has shown that the transverse disturbances created by the ship and wake motion will be almost completely attenuated using a cylindrical steel towing cable. Therefore, we need concern ourselves only with the longitudinal disturbances from these sources. Since the cable in the system we are considering forms a small angle with respect to the surface of the water, longitudinal disturbances due to ship and wake motion will be small. In our design we will consider their amplitude to be of the order of one or two inches. Larger disturbances could be handled merely by lengthening the VIM. The frequency of these disturbances will be on the order of a few cycles per second.

Lyon has also shown that boundary layer excitation tends to be broad-band with an upper frequency cutoff ( $f_c$ ) at  $6 \times 10^{-3} \frac{U_\infty}{D_c}$ .  $U_\infty$  is the velocity of tow and  $D_c$  is the cable diameter. The maximum value of  $U_\infty/D_c$  will be of the order of 500. Therefore  $f_c$  will be around 3 cps. The upper frequency limit which concerns us will be due to vortex shedding. The Strouhal number  $S$  which is proportional to the frequency of vortex shedding is given in Equation 1.

$$S = \frac{f D_c}{U_\infty} \quad (1)$$

In the Reynolds number range we are concerned with,  $S$  equals .21. Therefore, the maximum frequency will be of the order of  $10^2$  cps.

Disturbances from boundary layer excitation less than  $10^{-1}$  cps will probably not affect the performance of the towed body which is attached to the VIM; therefore, the VIM should be designed to attenuate disturbances in the frequency range from  $10^{-1}$  to  $10^2$  cps.

Since this frequency range covers three decades it will be necessary to have two spring constants, a small one to damp out low frequency disturbance and a large one to damp out the high frequencies.

- - - - -

(1) See page 1.

Any device which can prevent low frequency vibrations from reaching the towed body must have a very low resonance frequency, and must, therefore, have either a very low modulus or a very high effective mass. Since the mass is limited by the maximum possible size and mass of the tow, low resonance frequency can be achieved only by reduction of the modulus. However, since the isolation device must transmit the total towing force, provision of a low modulus leads to extreme elongations. These elongations can be troublesome in themselves and can also entail destructive hydroelastic instabilities. Some means of preserving a low modulus without high elongation is therefore desirable. It is obvious that this end cannot be attained through a purely passive device.

One means of achieving this objective is to balance the main towing effort in such a way that the attenuating spring carries only the fluctuation and not the active force. This balancing force can be provided either through a servomechanism or by a piston driven by the stagnation pressure. The present study is concerned with the latter principle. This is an acceptable approach, since both the stagnation pressure and drag force are proportional to the square of the towing velocity.

The preloading (due to the drag forces) imposed on the VIM is given by Equation 2.

$$F = \frac{1}{2} \rho U_{\infty}^2 S_w C_D \quad (2)$$

where

- $\rho$  = density of water ( $2\text{-lb}_f \text{ sec}^2/\text{ft}^4$ )
- $S_w$  = wetted area of tow body
- $C_D$  = drag coefficient of tow body ( $3 \times 10^{-3}$ )

For a tow body which is a circular cylinder with a radius of 1.5 inches and a length of 300 feet, the preloading  $F$  versus the tow velocity is given by Figure 2. Assuming a top design speed of 20 knots one gets a maximum preloading of  $750 \text{ lb}_f$ .



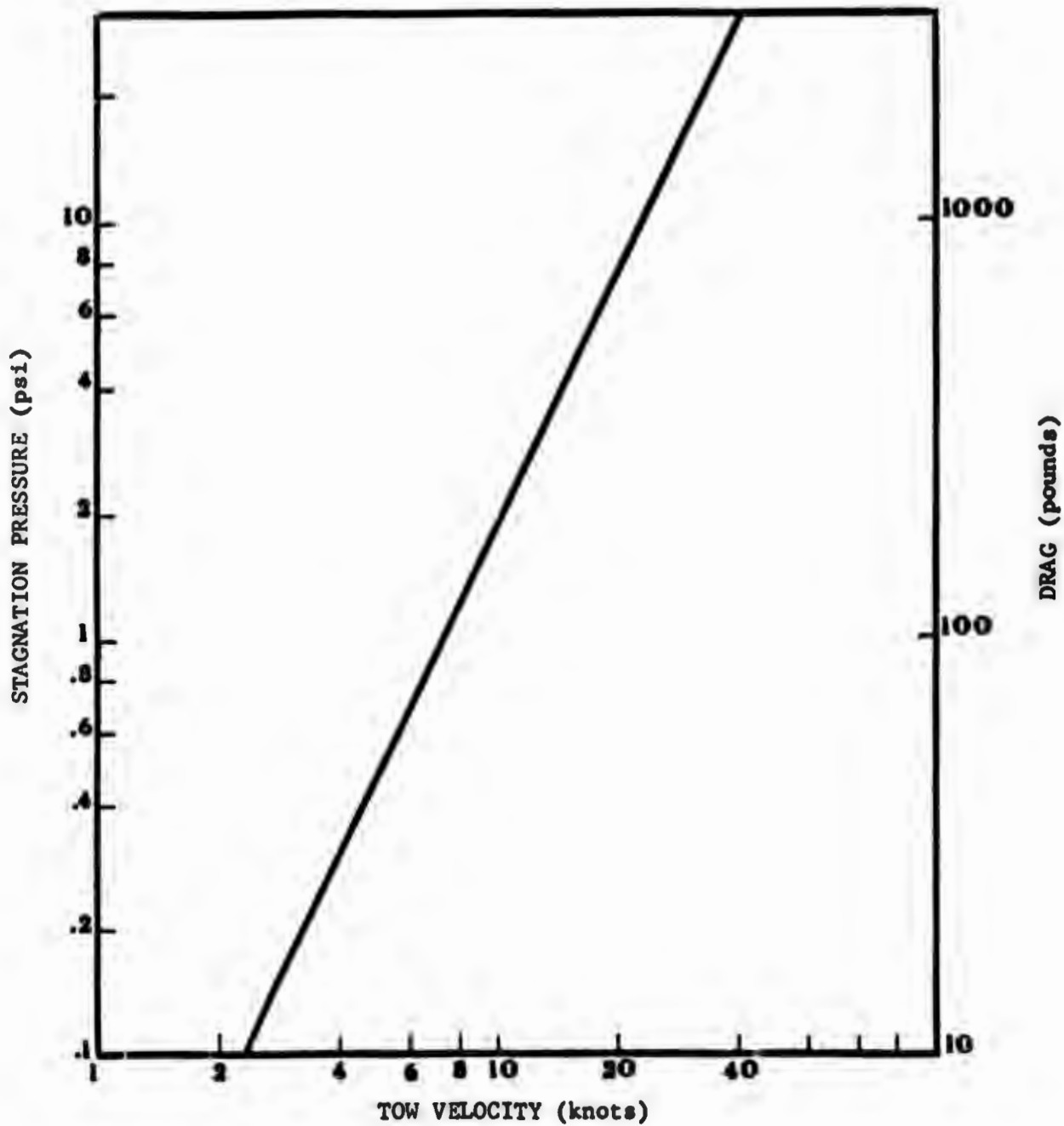


Fig. 2 - Stagnation pressure and drag vs. tow velocity for cylinder 300 ft. long and 3 in. in diameter

In the final design, the stagnation pressure in a scoop at the fore end of the VIM was converted, by means of a multiple piston arrangement, to a force which matched the drag of the towed body. Because the outside diameter of the VIM was limited to 4-1/2 inches, it was found necessary to use a stacked array of nine pistons, each fixed to a common pipe which served to supply water from the fore end scoop to nine individual compartments. These compartments were created by inserting a series of bulkheads and spacers into the common outside casing. Figure 3 shows the VIM in cross section.

The VIM was designed to be neutrally buoyant. This was accomplished through the use of low density plastic and aluminum. Design stress for all plastic parts was less than 600 psi. The fore and aft pistons were proportioned and positioned so that a fail-safe condition existed upon bottoming in either direction.

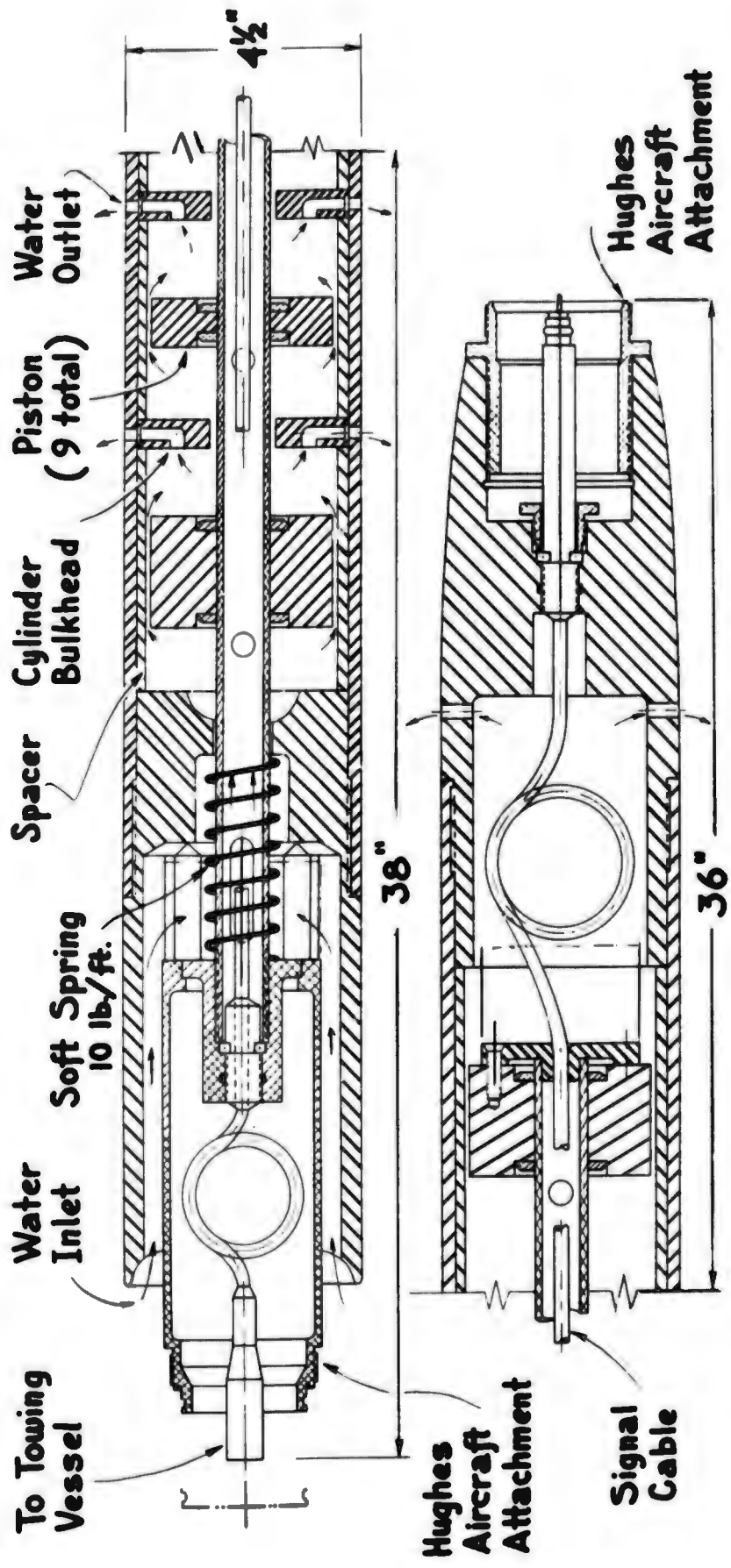


Fig. 3 - Prototype VIM in mid-stroke attitude.

### 3.0 THEORETICAL ANALYSIS

#### 3.0 Stability Analysis of a Conventional VIM

The usual construction for the vibration isolation mount is a section having very high elongation. It can be shown that this type of construction may be subject to static instability at high speeds.

To analyse it we will first assume that the spring force (which may not necessarily be linear) is in equilibrium with a towing effort which is given in Equation 3.

$$\frac{1}{2} \rho U_{\infty}^2 C_D 2\pi R l = f(l) \quad (3)$$

where:  $\rho$  = density of water

$U_{\infty}$  = towing velocity

$C_D$  = drag coefficient of the casing

$R$  = radius of the casing

$l$  = total length of casing

$f(l)$  = spring force at elongation  $l$

Let us now suppose that somewhere near the forward end of the towed body elongation is possible and that this elongation leads to a reduction of speed further back. We will further suppose that this elongation increases the wetted area and hence the drag. We will further suppose that there is an effect on the drag coefficient associated with a change from the purely cylindrical to some other distorted shape. Under these conditions Equation 3 will assume the form given in Equation 4.

$$\frac{1}{2} \rho U_{\infty}^2 \left(1 - \frac{2\xi}{U_{\infty}}\right) \left[ 2\pi R (l + \xi) C_D + 2\pi R (l + \xi) \frac{\partial C_D}{\partial l} \xi \right] = f(l) + \xi \frac{\partial f}{\partial l} \quad (4)$$

Here  $\xi$  is the elongation of the VIM.

Equation 4 may be rearranged and the non-linear terms can be dropped. This will lead to Equation 5.

$$\frac{1}{2} \rho U_{\infty}^2 \left[ \left(1 - \frac{2\xi}{U_{\infty}}\right) 2\pi C_D R l + 2\pi C_D R \xi + 2\pi R l \frac{\partial C_D}{\partial l} \xi \right] = f(l) + \frac{\xi \partial f}{\partial l} \quad (5)$$

Recalling Equation 3 we see that Equation 5 reduces to

$$\rho U_{\infty}^2 \left[ \frac{-2\pi C_D R l \dot{\xi}}{U_{\infty}} + \pi C_D R l \left( \frac{\xi}{l} + \frac{1}{C_D} \frac{\partial C_D}{\partial l} \xi \right) \right] = \frac{\xi \partial f(l)}{\partial l} \quad (6)$$

If we divide Equation 6 by the mean towing effort it will reduce to the form given in Equation 7.

$$\frac{-2\dot{\xi}}{U_{\infty}} + \left( \frac{1}{l} + \frac{1}{C_D} \frac{\partial C_D}{\partial l} \right) \xi = \xi \frac{\partial f}{\partial l} / \pi C_D R l \rho U_{\infty}^2 \quad (7)$$

Equation 7 can be rewritten as

$$\frac{2\dot{\xi}}{U_{\infty}} = \left[ \frac{1}{l} + \frac{1}{C_D} \frac{\partial C_D}{\partial l} - \frac{1}{f(l)} \frac{\partial f}{\partial l} \right] \xi \quad (8)$$

We will note that in both Equations 7 and 8 the denominator in the last term will be equal to the towing effort. This will facilitate a physical discussion of behavior of this device.

To solve Equation 8 we will make the substitution given in Equation 9.

$$\xi = \bar{\xi} \exp[\alpha U_{\infty} t / l] \quad (9)$$

where  $\alpha$  is a constant to be determined. Stability will depend upon the sign of  $\alpha$ , a positive value being unstable and a negative value stable. If we substitute 9 into 8 we obtain the relationship given in Equation 10.

$$\alpha = \frac{1}{2} \left[ 1 + \frac{l}{C_D} \frac{\partial C_D}{\partial l} - \frac{Kl}{f(l)} \right] \quad (10)$$

In this relationship  $K$  is the spring constant of the VIM.

If we suppose that there is no distortion of the outer shape on elongation then we will require, for stability, that the relationship in Equation 11 be satisfied.

$$\frac{Kl}{f(l)} > 1 \quad (11)$$

If we assume that the towed body is 300 ft. long and that the total load is 700 lbs., then, for stability, the spring constant must be greater than  $7/3$  of a pound. In our analysis (Section 3.3) of the isolation characteristics of the VIM we found that five pounds is necessary to procure adequate isolation for the low frequencies which might be present. If we assume that there is no change in the drag coefficient, this is fairly close to the conditions of instability and a surge such as one might expect in a wake could very well create divergence. In actual fact the drag coefficient will usually be an increasing function with elongation since there will be distortions of various types. For example, it may readily be shown that in a simple corrugated construction this change will be quite large. As a result the spring constant of five lb/ft is probably too small to assure stability within a reasonable factor of safety. There are several added consequences which derive from the relationship in Equation 10. If the body is so designed that there is no elongation at all aft of the spring and consequently no change in drag coefficient aft of the spring, then the condition for stability will always be satisfied since the variations in total drag which lead to instability will be absent. This result will lead to the following principle in designing a spring section covered by a sleeve. If we wish stability, the external sleeve must be aft of the spring so that the drag coefficient of the moving portion does not change on elongation. If the external sleeve is in the forward portion then as the aft portion withdraws from the sleeve the drag coefficient will increase and instability may ensue. This principle has been observed in the design which we propose for the section with a low spring constant.

### 3.2 Principle of Action of Proposed VIM

The high preloading precludes the possibility of having two spring-mass systems in series, since the spring with the low spring constant would be highly elongated. This condition tends toward instability because the drag force increases with increasing length of any part of the system.

Figure 4 gives a schematic representation of a VIM utilizing the dynamic pressure to balance the drag force on the spring with the small spring constant. (Other designs which were considered will be discussed in the Appendix of this report.)

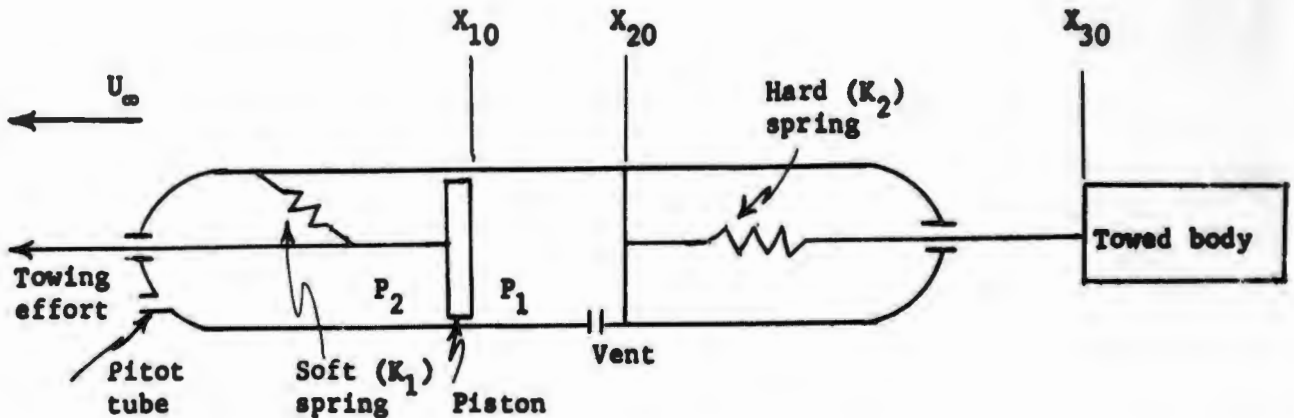


Figure 4. Schematic Representation of VIM

If we examine Figure 4 we see that the forces on the main body of the VIM have three sources. The forward motion is provided by the pressure in the cylinders and by the spring. This motion is resisted by the body drag and by the inertia. As a consequence we will obtain Equation 12.

$$P_D C_D S_w - (P_2 - P_1)A \cdot g(e) = M_E \dot{U}_2 \quad (12)$$

where  $M_E$  is the effective mass of the VIM plus towed body

$U_2$  is its velocity

$P_D$  is the dynamic pressure

$C_D$  is the drag coefficient of the towed body

$A$  is the area of the piston in the VIM

$S_w$  is the wetted area

$P_1$  is the ambient pressure

$P_2$  is the pressure shown in the cylinder

$g(e)$  is a function of the elongation,  $e$ , expressing the force of the spring.

If we collect all terms on the left hand side of the equation we will obtain the relation given in Equation 13.

$$P_D C_D S_w - (P_2 - P_1)A - g(e) - M_E \dot{U}_2 = 0 \quad (13)$$

Let us now examine the nature of the pressure ( $P_2$ ) in the cylinder. This will be determined by two separate factors. One will be the stagnation pressure ( $P_0$ ) and the other will depend upon the motion of the piston. If the piston is fixed then  $P_2$  will depend only on the stagnation pressure and on the past history of the stagnation pressure. If there is no mechanism for a time delay between a buildup of the pressure in the cylinders and the buildup of stagnation pressure then, when the piston is fixed, these two will be identical. If  $P_0$  is held constant the pressure  $P_2$  will depend upon the motion of the pistons and the ease with which the water flows in and out. If we confine ourselves to linear effects then  $P_2$  must consequently have the general form given in Equation 14.

$$P_2 = Z_1(D)P_0 - Z_2(D)De \quad (14)$$

Here  $Z_1$  and  $Z_2$  are differential operators of  $D$  which is differentiation with respect to time. The time derivative of the elongation  $e$  is given by Equation 15.

$$\dot{e} = U_1 - U_2 = De \quad (15)$$

where  $U_1$  and  $U_2$  are respectively the velocities of one and the other forward sections of the tow. Let us further suppose that the forward section is subject to a velocity fluctuation such that Equation 16 is satisfied.

$$U_1 = U_\infty + u \quad (16)$$

Using the relationships in 15 and 16 we will obtain Equations 17 and 18 for the velocity and the dynamic pressure respectively.



$$U_2 = U_1 - \dot{e} = U_\infty + u - \dot{e} \quad (17)$$

and

$$P_D = \frac{1}{2} \rho U_2^2 = \frac{1}{2} \rho U_\infty^2 \left( 1 + \frac{2u}{U_\infty} - \frac{2\dot{e}}{U_\infty} \right) \quad (18)$$

where we have dropped quadratic terms in  $u$  and  $\dot{e}$ . Let us now make the substitution given in Equation 10.

$$\begin{aligned} \dot{\theta} &= \frac{u}{U_\infty} - \frac{\dot{e}}{U_\infty} \\ \dot{\eta} &= \frac{u}{U_\infty} \\ \frac{1}{2} \rho U_\infty^2 &= q \end{aligned} \quad (19)$$

Then, since  $P_0 = P_1 + P_D$ , the equation of motion becomes

$$C_D S_w q (1 + 2\dot{\theta}) - A \left[ Z_1 (P_D + P_1) - Z_2 (\dot{\theta} - \dot{\eta}) - P_1 \right] - g(e) - M_E U_\infty \ddot{\theta} = 0 \quad (20)$$

Assuming that  $P_1$  is constant and that  $g(e)$  can be expanded in a Taylor series we get

$$\begin{aligned} C_D S_w q (1 + 2\dot{\theta}) - A \left[ Z_1 q (1 + 2\dot{\theta}) - Z_2 (\dot{\theta} - \dot{\eta}) \right] - g(e) - f'(e_0) - f'(e_0) (\theta - \eta) \\ - M_E U_\infty \ddot{\theta} = 0 \end{aligned} \quad (21)$$

dropping terms higher than the first degree.

If we assume that the static forces are balanced separately, we will obtain

$$C_D S_w q - A Z_0 q - f(e_0) = 0 \quad (22)$$

The dynamic balance will then be achieved by setting equal to 0 the terms in Equation 22 which depend on  $\theta$  and  $\eta$ . Isolating these two variables on the left and right hand sides of the equation respectively we

obtain the relationship given in Equation 23.

$$\left[ 2q(C_D S_w - AZ_1) + AZ_2 \right] \dot{\theta} - f'(e_o) \dot{\theta} - M_E U_w \ddot{\theta} = AZ_2 \dot{\eta} - f'(e_o) \dot{\eta} \quad (23)$$

It is clear from the definition of the quantities that the motion of the main body of the VIM is proportional to  $\theta$ . The quantity  $\eta$  on the other hand is proportional to the motion of the forward section of the VIM. The ratio of  $\theta/\eta$  is therefore a measure of the effectiveness of the VIM. If this ratio is small the VIM will be effective, if it is not small but approaches 1 the VIM will be ineffective.

If there is no time delay between the stagnation pressure and the pressure in the cylinder when the pistons are held fixed, then  $AZ_1$  will simply be a constant. In this case we would choose A, the area of the pistons, so that the parenthesis multiplying q vanishes. In this case it may readily be seen that the system behaves as an oscillating system in which the mass  $M_E$  is the mass of the body including the added mass due to the fluid, the spring constant is present and there is a dashpot effect. The effective mass of the circulating water is included in the expression for  $Z_2$  which, in the simplest case, will be a first degree linear operator:  $Z_2 = (B + C \frac{d}{dt})$ . It is physically obvious that the factor in the damping present in  $Z_2$  must be large compared to the effect of the stagnation pressure on the motion of the piston. If this were not the case it would be possible to construct a system which, once set in motion, would continue indefinitely. This would obviously violate the law of conservation of energy. Using this conclusion it is not difficult to show that the system will always be stable.

### 3.3 Discussion of Vibration Transfer Function of VIM

As shown in the previous Section, the force  $(P_2 - P_1)A$  (which is equal to  $\frac{1}{2} \rho U_w^2 A$ ) may be made equal to the towing force  $\frac{1}{2} \rho U_w^2 C_D S_w$  by a suitable choice of A. Therefore A will equal  $C_D S_w$ .

Since the towing force is equal to the pressure force on the piston, an equilibrium position will be reached by the piston such that the soft

spring is in its neutral position. The hard spring will also have an equilibrium position such that the product of its elongation and its spring constant is equal to the towing force. Consequently, we have a mass-spring system with a soft spring to damp out low frequency disturbances and a hard spring to damp out high frequency disturbances.

For disturbances to be attenuated it is necessary that the transmissibility ratio  $X_3/X_1$  (measured from the equilibrium positions shown) be less than one. Whether this behavior will occur depends upon the ratio of the inertia of the towed body to the inertia of the masses in the VIM, the spring constants and the time constants of the apertures in the VIM. It has already been shown that the proposed VIM should be stable so therefore a simplified analysis is presented here to determine the magnitude of the spring and dashpot constants required to achieve the necessary attenuation.

Assuming that the only forces acting on the system displaced from an equilibrium position are those arising from the two springs, we have formulated the problem using Lagrange's Equation.

$$\frac{d}{dt} \left( \frac{\partial T}{\partial \dot{X}_j} \right) - \frac{\partial T}{\partial X_j} = Q_j \quad (24)$$

$$Q_j = -\frac{\partial V}{\partial X_j} + \delta_{j1} h(t) \quad (25)$$

In Equations 23 and 24  $T$  is the kinetic energy,  $V$  is a potential energy function,  $\delta_{j1}$  is the Kronecker delta ( $\delta_{j1} = 1$  when  $j = 1$ ;  $\delta_{j1} = 0$  when  $j \neq 1$ ) and  $h(t)$  is a forcing function acting on the piston in the VIM.

The kinetic energy  $T$  is given by Equation 26.

$$T = \frac{1}{2} \left[ M_1 \dot{X}_1^2 + M_2 \dot{X}_2^2 + M_3 \dot{X}_3^2 \right] \quad (26)$$

where  $X_1$  = displacement from equilibrium position,  $X_{10}$  shown in Figure 4 and  $\dot{X}_1 = \frac{dX_1}{dt}$ .

- $M_1$  = mass of piston
- $M_2$  = effective mass of VIM
- $M_3$  = effective mass of towed body

We are assuming that the springs are massless and that added mass terms due to fluid moving through the various openings are negligible. An analysis of another system (see Appendix) has shown that the added masses can be ignored.

The potential energy term is given by Equation 27.

$$V = \frac{1}{2} K_1 (X_1 - X_2)^2 + \frac{1}{2} K_2 (X_2 - X_3)^2 \quad (27)$$

where

- $K_1$  = spring constant of soft spring
- $K_2$  = spring constant of hard spring.

Substituting Equation 26 and Equation 27 into Lagrange's Equation we get the following three equations of motion.

$$M_1 \ddot{X}_1 = -K_1 X_1 + K_1 X_2 + h(t) \quad (28)$$

$$M_2 \ddot{X}_2 = K_1 X_1 - (K_1 + K_2) X_2 + K_2 X_3 \quad (29)$$

$$M_3 \ddot{X}_3 = K_2 X_2 - K_2 X_3 \quad (30)$$

Let us take the Fourier transform of  $h(t)$  and  $X_1(t)$ . Substituting this into Equations 27, 28 and 29 we get three simultaneous equations in  $\bar{X}_1$  and  $\bar{h}$ , where

$$\begin{aligned} \bar{X}_1 &= \int_{-\infty}^{\infty} X_1(t) \exp[-i\omega t] dt \\ \bar{h} &= \int_{-\infty}^{\infty} h(t) \exp[-i\omega t] dt \end{aligned} \quad (31)$$

and the frequency  $\omega$  is related to the real frequency  $f$  by the relation  $\omega = 2\pi f$ .

$$-\omega^2 M_1 \bar{x}_1 = -K_1 \bar{x}_1 + K_1 \bar{x}_2 + \bar{h} \quad (32)$$

$$-\omega^2 M_2 \bar{x}_2 = K_1 \bar{x}_1 - (K_1 + K_2) \bar{x}_2 + K_2 \bar{x}_3 \quad (33)$$

$$-\omega^2 M_3 \bar{x}_3 = K_2 \bar{x}_2 - K_2 \bar{x}_3 \quad (34)$$

Solving for the ratio  $\bar{x}_3 / \bar{x}_1$  we get

$$\frac{\bar{x}_3}{\bar{x}_1} = \frac{K_1 K_2}{(K_2 - \omega^2 M_3) (K_1 + K_2 - \omega^2 M_2) - K_2^2} \quad (35)$$

Equation 35 can be written as

$$\bar{x}_3 = W(i\omega) \bar{x}_1 \quad (36)$$

where  $\bar{x}_3$  is the transform of the steady-state response of the system to a periodic input  $x_1$ .  $W(i\omega)$  is a characteristic of the system (i.e. the VIM) regardless of the form of the input. For an input of the form  $\exp[i\omega t]$

$$x_3(t) = \exp[i\omega t] W(i\omega) \quad (37)$$

If we write  $W(i\omega)$  in polar form, Equation 37 can be written as

$$x_3(t) = \left| W(i\omega) \right| \exp[i(\omega t + \psi)] \quad (38)$$

Therefore  $W(i\omega)$  is the ratio of the output amplitude to the input amplitude. Since the system is linear, the relation holds for any input amplitude. The determination of the attenuation of our system, therefore, reduces to finding the magnitude of  $W(i\omega)$ .

Since both the towed body and the VIM are to be neutrally buoyant the calculation of  $M_2$  and  $M_3$  is straightforward knowing the dimensions

of each body. The towed body is a circular cylinder (radius = R) of length  $L_0$  and the VIM is also designed to be a circular cylinder (radius = r) of length  $l_0$ . Therefore

$$M_2 = \pi r^2 l_0 \rho_w \quad (39)$$

and 
$$M_3 = \pi R^2 L_0 \rho_w \quad (40)$$

The spring constants can be written in complex form

$$K_j = K_j' + i\omega c_j ; j = 1, 2 \quad (41)$$

where

$k_j'$  = normal spring constant

and

$c_j$  = normal dashpot constant.

Substituting Equations 39, 40, and 41 into Equation 34 we get for the transmissibility ratio  $X_3/X_1$ , Equation 42

$$\frac{X_3}{X_1} = \frac{a + ib}{c + id} \quad (42)$$

where

$$a = K_1' K_2' - \omega^2 c_1 c_2$$

$$b = \omega c_1 K_2' + \omega c_2 K_1'$$

$$c = K_1' K_2' - \omega^2 [c_1 c_2 + (\pi r^2 l_0 \rho_w + \pi R^2 L_0 \rho_w) K_2' + \pi R^2 L_0 \rho_w K_1' - \omega^2 \pi^2 \rho_w^2 R^2 r^2 L_0^2 l_0^2]$$

$$d = \omega [c_1 K_2' + c_2 K_1' - \omega^2 \{c_2 \pi \rho_w (r^2 l_0 + R^2 L_0) + c_1 \pi \rho_w R^2 L_0\}]$$

The magnitude of  $X_3/X_1$  can now be tabulated for various values of  $K_1'$ ,  $K_2'$ ,  $c_1'$ ,  $c_2'$ , r,  $l_0$ , R,  $L_0$ . The results are given in Table I.

TABLE I  
Frequency vs. Transmissibility Ratio

Frequency ( $\omega$ )		Transmissibility Ratio $ X_3/X_1 $										
rad/sec	cycles/sec	#1	#2	#3	#4	#5	#6	#7	#8	#9	#10	#11
.3	.0478	1.360	1.356	1.260	1.256	1.170	1.170	1.158	1.154	1.593	2.018	1.394
.4	.0637	1.731	1.719	1.383	1.374	1.340	1.331	1.290	1.282	1.607	2.699	1.949
.5	.0796	2.122	2.098	1.410	1.398	1.621	1.603	1.460	1.445	1.217	1.429	3.273
.6	.0955	1.907	1.896	1.316	1.304	2.089	2.048	1.636	1.611	.883	.811	3.094
.7	.1115	1.354	1.355	1.160	1.150	2.721	2.646	1.729	1.697	.675	.542	1.572
.8	.1275	.967	.970	1.004	.996	2.767	2.730	1.659	1.629	.542	.400	.956
.9	.143	.731	.734	.871	.864	2.010	2.026	1.460	1.440	.453	.314	.658

Example	$K_1'$ lb <sub>f</sub> /ft	$K_2'$ lb <sub>f</sub> /ft	$C_1$ lb <sub>f</sub> sec/ft
1	10	500	10
2	10	1000	10
3	10	500	20
4	10	1000	20
5	20	500	10
6	20	1000	10
7	20	500	20
8	20	1000	20
9	5	1000	10
10	5	1000	5
11	10	1000	5

For all examples:  $C_2 = 1 \text{ lb}_f\text{sec/ft.}$

$r = .2 \text{ ft.}$

$R = .125 \text{ ft.}$

$A_0 = 10 \text{ ft.}$

$L_0 = 300 \text{ ft.}$

Design considerations did not allow much variation in the values of  $r$  and  $h_0$ . Preliminary work showed that they had to be around 2-2.5 inches and 10 feet respectively. Because of this they would have little effect on the magnitude of  $X_3/X_1$ . Consequently it was decided to hold them constant in our numerical analysis. From physical considerations the dashpot constant  $c_2$  should be small so as not to affect  $K_2'$ . It was found that  $c_2$  could be held constant and equal to unity without seriously affecting our results. Therefore, we only had to study the variation in  $K_1'$ ,  $K_2'$  and  $c_1$ . As seen from Table I, satisfactory results were obtained for example #10, where  $K_1' = 5$ ,  $K_2' = 1000$ , and  $c_1 = 5$ . A plot of  $|X_3/X_1|$  vs.  $\omega$  was made for these values of  $K_1'$ ,  $K_2'$ , and  $c_1$  (see Figure 5). For  $\omega$  greater than .75  $|X_3/X_1|$  is less than .5 which means that the attenuation is greater than 50%. In the neighborhood of  $\omega = 10$   $|X_3/X_1|$  goes through a minimum. It reaches a second resonance at  $\omega = 20$ . However, this peak is less than .1 so that the attenuation is greater than 90%.

We can conclude therefore that with values of  $K_1' = 5$ ,  $K_2' = 1000$  and  $c_1 = 5$  satisfactory attenuation can be achieved in the frequency range from  $10^{-1}$  to  $10^2$  rad/sec.

### 3.4 Effect of Bladder on VIM Performance

Up to now we have assumed that the equations of motion were influenced by two operators  $Z_1$  and  $Z_2$  of which we did not specify the nature. We will now calculate these operators. The pressure difference between the scoop and the cylinder, assuming only one cylinder, will be proportional to the rate of flow operated on by a linear operator which is usually of the first order. Thus we will have Equation 43.

$$(P_0 - P_2) = Z_3 \bar{v} = (a_g + b_g D) \bar{v} \quad (43)$$

Here  $a_g$  is the frictional term in the flow between the scoop and cylinder and  $b_g$  the inertial term. To complete the calculation it is necessary to consider the change in volume. If the only change in volume in the cylinder is due to the motion of the piston, then the total volume will be a linear function of  $e$  alone. If we assume the presence of a bladder or



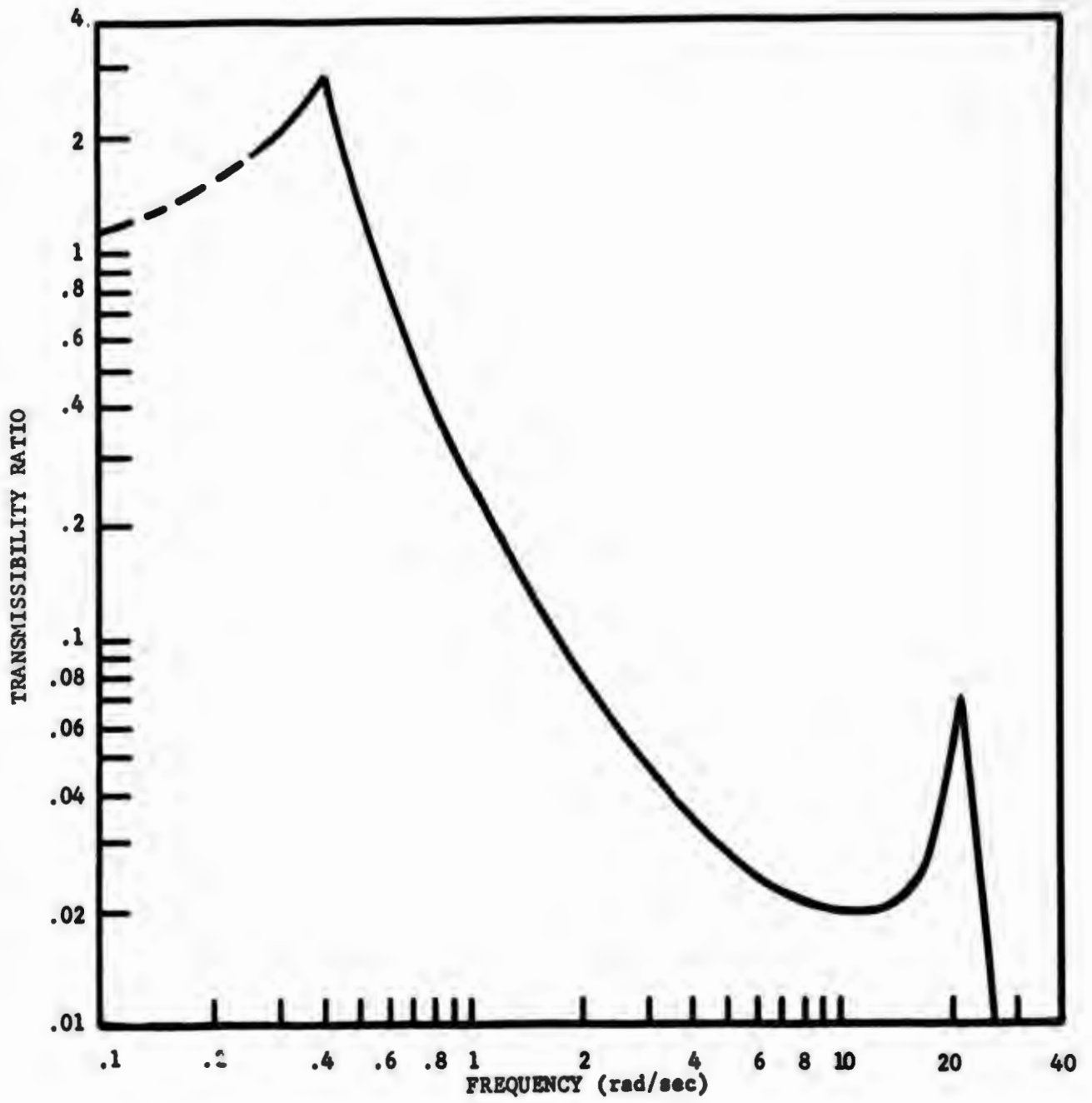


Fig. 5 - Transmissibility ratio vs. frequency  
 $(K_1' = 5, K_2' = 1000, \text{ \& } c_1 = 5)$

some device which changes volume with pressure, then we will have the more general relationship for the volume which is given in Equation 44.

$$V_1 = kP_2 + V_0 + Ae \quad (44)$$

Now the time rate of change of the volume must be equal to the inflow of fluid from the scoop. Consequently we must have Equation 45.

$$\dot{V}_1 = k\dot{P}_2 + A\dot{e} = \bar{v} \quad (45)$$

Combining Equations 43 and 45 we obtain the relationship given in Equation 46.

$$P_0 = (1 + kZ_3D)P_2 + AZ_3De \quad (46)$$

Solving for  $P_2$  we get

$$P_2 = \frac{(P_0 - AZ_3De)}{(1 + kZ_3D)} \quad (47)$$

This will finally lead to the relationships given in Equation 48 for  $Z_1$  and  $Z_2$ .

$$\begin{aligned} Z_1 &= \frac{1}{(1 + kZ_3D)} \\ Z_2 &= \frac{AZ_3}{(1 + kZ_3D)} \end{aligned} \quad (48)$$

Substituting these expressions for  $Z_1$  and  $Z_2$  into Equation 23 and assuming that the time independent terms of the forces induced by the flow through the drag and through the pressure cylinders cancel (i.e.  $A = C_D S_w$ ) we get Equation 49.

$$\left[ \frac{C_D S_w Z_3 (2qkD + A)D}{(1 + kZ_3D)} - f' - M_E U_w D^2 \right] \theta = \left[ \frac{C_D S_w AZ_3 D}{(1 + kZ_3D)} - f' \right] \eta \quad (49)$$

In Equation 49 we have assumed that the static terms cancel. If we make the special assumption that the inertial forces may be neglected in the motion of the fluid through the pipe then

$$\left[ \frac{2C_{Dw} S_w q \tau D^2 + C_{Dw} S_w A/k \tau D}{(1 + \tau D)} - f' - M_E U_\infty D^2 \right] \theta = \left[ \frac{C_{Dw} S_w A}{k} \frac{\tau D}{(1 + \tau D)} - f' \right] \eta \quad (50)$$

where  $\tau$  is the relaxation time. If we take the Fourier transform and solve for  $\theta/\eta$  we will finally obtain Equation 51.

$$\frac{\theta}{\eta} = \frac{\frac{iC_{Dw} S_w A \tau \omega}{k(1 + i\tau\omega)} - f'}{-2C_{Dw} S_w q \tau \omega^2 + \frac{iC_{Dw} S_w A \tau \omega}{k} - f' + M_E U_\infty \omega^2} \quad (51)$$

In this relation we see that at low frequencies there is an additional effective mass resisting change in motion of the towed body. It is of interest to compare the force attributable to this mass to that attributable to the mass of the towed body. For this purpose we compare the magnitude of the two expressions by taking their ratio. This is given by

$$\frac{M_E U_\infty}{2C_{Dw} S_w q \tau} \quad (52)$$

Expressing the various quantities in terms of the dimensions of the towed body we will obtain

$$\frac{M_E U_\infty}{2C_{Dw} S_w q \tau} = \frac{\gamma R}{2U_\infty \tau C_D} \quad (53)$$

where  $\gamma$  is a coefficient whose value is usually close to one and which expresses the effect of the added mass. If we introduce reasonable numbers into this relationship, we find that the two masses will be of the same order of magnitude when the relaxation time is of the order

of magnitude of one second.

At high frequencies we find that the additional mass disappears and that the total assembly behaves as if it were a mass-spring combination. The entire effect of the inclusion of this type of bladder is uncertain and should be studied before deciding whether to include this feature and how large the resulting coefficients should be.

## 4.0 DESIGN AND CONSTRUCTION OF MODEL

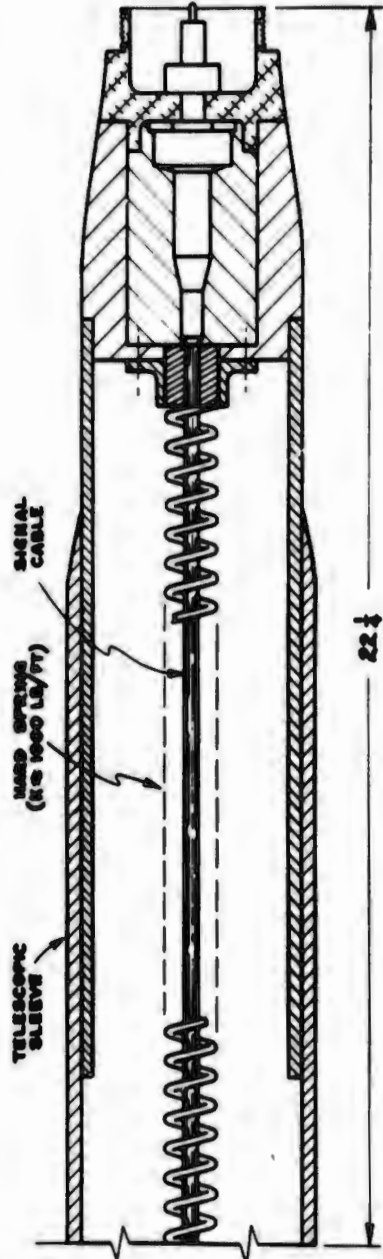
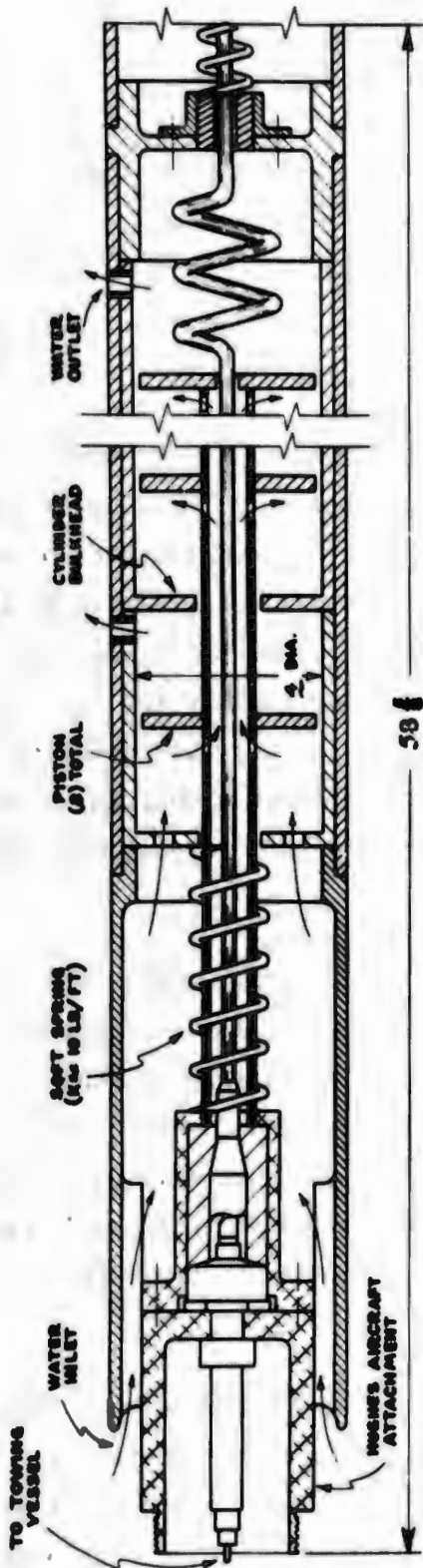
### 4.1 Design Analysis

Figure 6 is a design of a functional VIM which meets the basic theoretical requirements. It is based on the use of a stacked piston array in which each piston is acted on by the dynamic pressure. The pistons are attached to a common rod and the sum of the forces acting on the pistons acts to balance the drag force of the towed body attached to the VIM.

The objective of subjecting the individual pistons to the dynamic pressure is achieved by building multiple bulkheads into the body of the VIM and using a hollow piston-rod to allow water to flow into the bulkhead compartments. In this way, one side of each piston is vented to the ambient pressure and the other to the stagnation pressure. Since water leakage is not critical, liberal clearances are permissible for the piston fits in the body and the piston-rod fit through the multiple bulkheads. This assures relatively high reliability as compared to a unit in which leak-proof seals are required, such as for the hydraulic amplifying type described in the Appendix of this report.

Telescoping arrangements having low frictional properties are provided in the forward and aft sections of the VIM. The forward section which attaches to the ship cable is attached to the internal piston rod heretofore described and is free to move within the front section of the VIM. This front section has water inlet ports communicating with a scoop. The aft section of the VIM is connected to one end of the hard spring and is free to move, relative to the VIM midsection, when the tow force changes.

The VIM is designed to damp out vibrations in a range of known frequency and amplitude. In an idealized operating state the equilibrium position of the piston array is such that the individual pistons are at the centers of their respective chambers. In actual practice this probably will not be the case, since the drag force of the towed body will not exactly match the total effective piston forces. Therefore, the



GEN'L NOTE VIA SHOWN IN MID-STROKE ATTITUDE

Fig. 6 - Conceptual design of VIM

optimum length and compression state of the soft spring and the piston array travel will be determined from combined theoretical and experimental studies.

The coiled signal cable attached to forward and aft sections allows relative movement between these sections. Special fittings matching the Hughes Aircraft attachment are provided.

#### 4.2 Choice of Materials

Various metal alloys, hard organic plastics and other materials were considered for use in the body and miscellaneous parts of the VIM. Included were: stainless steel, aluminum, glass-fiber-reinforced plastic, ABS plastic, PVC and polypropylene. The latter is recommended since it offers a good balance of physical properties, is practically unaffected by sea water, and has a specific gravity of .92 which offers the greatest flotation rating. The design working stress of this material would be 600 psi, which at 50°F represents a safety factor of about 10.

ABS plastic with a specific gravity of about 1.1 is the second choice in the plastic group. Use of this material would result in a 10 to 15% increase in overall length of the VIM.

Aluminum alloys having adequate physicals are available for use in salt water. However, the overall length of the VIM would be about double that for the case of polypropylene. Possibly, the length could be reduced by the use of a suitable flotation material such as syntactic foam but this has not been considered in detail.

Selection of materials for the springs is to be based on design requirements for space, spring forces and end connection details. High alloy steel and syntactic rubber are being considered.

#### 4.3 Construction of Model

The test model was constructed in the shops at the Research Center. The various sections of the external case and the bulkhead spacers were

constructed from extruded seamless polypropylene pipe. The pistons, bulk-heads, and adapter flanges were machined from extruded polypropylene rod stock. The hollow piston rod for the piston array was made of aluminum (6061T6). The snap rings were stainless steel. Threaded connections fore and aft make it possible to change the springs and to make cable connections. Provision was made for accomodating the signal cable and for sealing around it.



## 5.0 VIBRATION TESTS

### 5.1 Test Apparatus

The VIM was rigidly mounted in a water tank by means of an adapter fitted to the aft end. The tank containing the VIM was suspended by a cable harness and was "grounded" to a variable-position take-up through a hard spring (1000 lb/ft). This spring attenuated vibrations in the high frequency range (800-1200 cps). A dynamometer mounted on the take-up measured the total force transmitted through the VIM.

The oscillator consisted of a stepless, variable-speed motor having an eccentric bushing and a crank arm assembly. The amplitude of the vibrations produced was 0.040 inch and the frequency range was from 1 to 17 cycles per second.

Figure 7 is a schematic presentation of the test set-up.

To facilitate introduction of water into the system, the front section of the VIM was modified by replacing the Hughes Aircraft attachment with a pipe and nipple combination so as to extend the piston pipe beyond the fore end of the VIM body. This extension was connected to the mechanical oscillator through a drive rod and also to a supply tank by means of a flexible hose. The supply tank was connected to an ordinary water line. During tests, an air space was maintained in the top of the supply tank as shown in the figure.

Two means of measuring the attenuating capability of the VIM were employed. These were a direct-reading dial indicator (shown in Figure 7) or a linear potentiometer-recorder (not shown).

### 5.2 Test Results

In a preliminary experiment the force-generating capacity of the VIM was determined in the pressure range from very low up to 15 psi gauge. In agreement with design calculations, the force factor (K) was found to

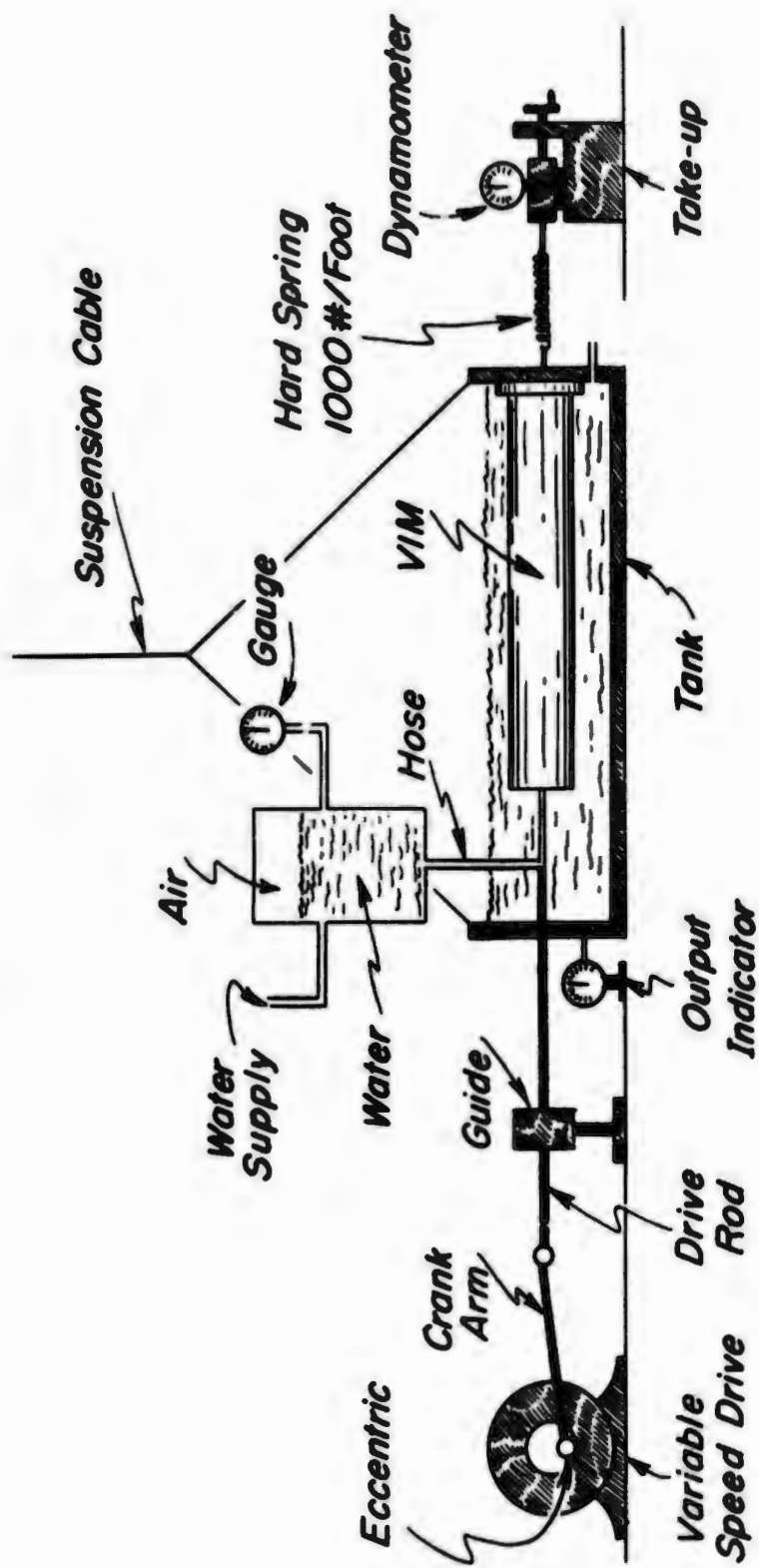


Fig. 7 - Test apparatus

be of the order of 90, i.e., for a gauge reading of 5 psi the force developed was approximately 450 pounds. For these tests, the radial piston clearance was .0025 inch. Figure 8 shows the relation between total water flow and the force developed by the nine tandem pistons.

Testing was then begun to determine the attenuating properties of the VIM. In the very first trials it became apparent that friction forces in the system were excessive, as evidenced by lock-in of the VIM to the oscillator throughout the frequency spectrum employed. A program was therefore started to reduce friction to an acceptable level. The first change was to increase the radial piston clearance to about .020 inch. This resulted in a reduction in friction force, but the force amplification was lowered to an unsatisfactory level due to the large increase in water flow and the resulting pressure gradient from the first to the ninth compartment.

A screening program was then initiated to search for a low-friction, low-leakage seal. Included in this program was an evaluation of each of the following:

- Formed lips on pistons
- Standard "O" rings
- Mylar film rings
- Felt rings
- Polypropylene piston rings
- Jar rings
- L rings
- Hollow "O" rings

The last four of the above list are shown in Figure 9. The hollow "O" ring made from soft rubber tubing and inserted in a wide groove gave the best performance relative to friction, although leakage remained a problem in that a substantial drop in force amplification resulted.

A test run to measure the damping properties of the VIM was made using a modified piston array in which only three pistons were used. Using this approach it was possible to reduce friction to a value

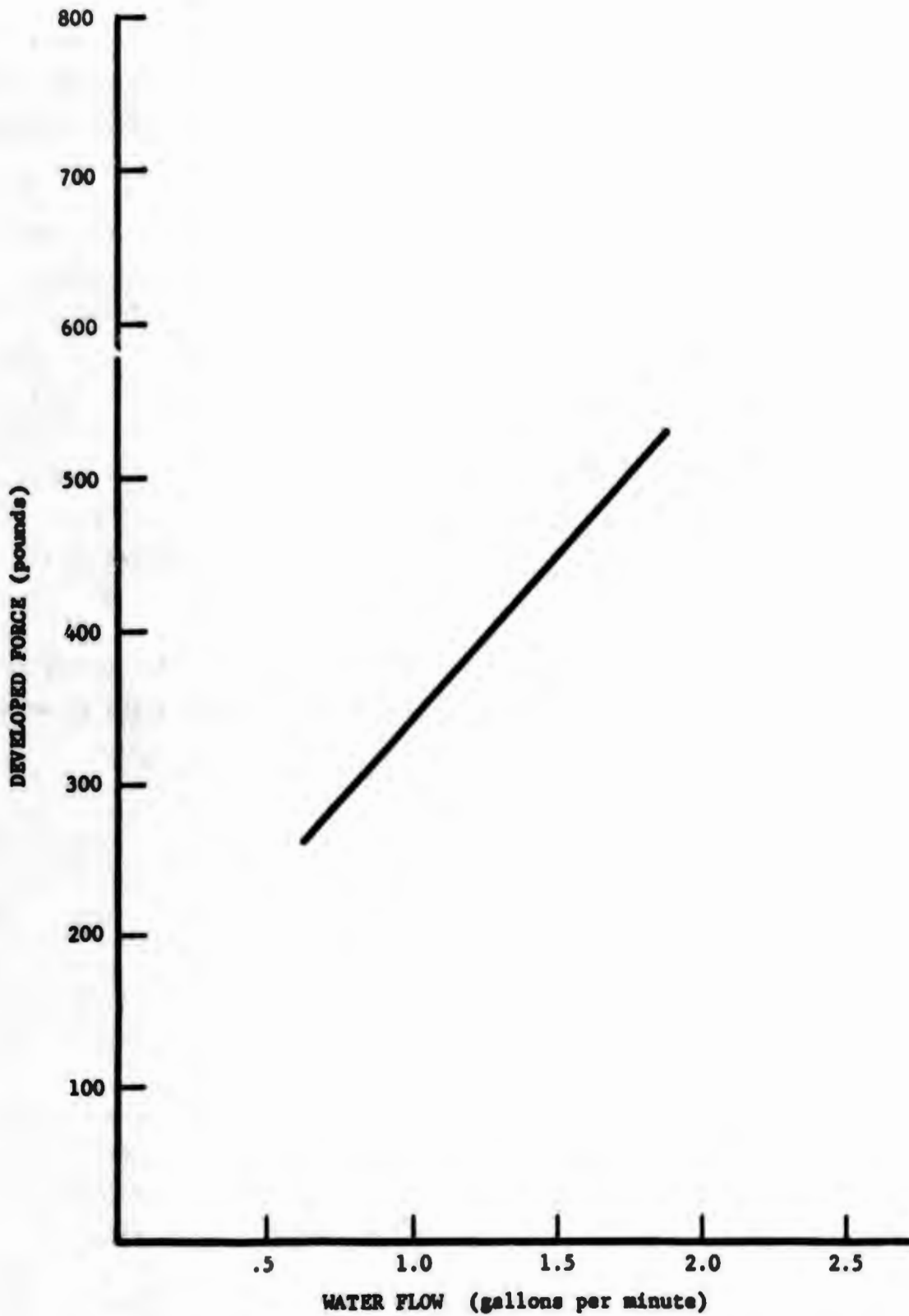


**Fig. 8 - Force-generating capacity of VIM  
(radial piston clearance = .0025 inch)**

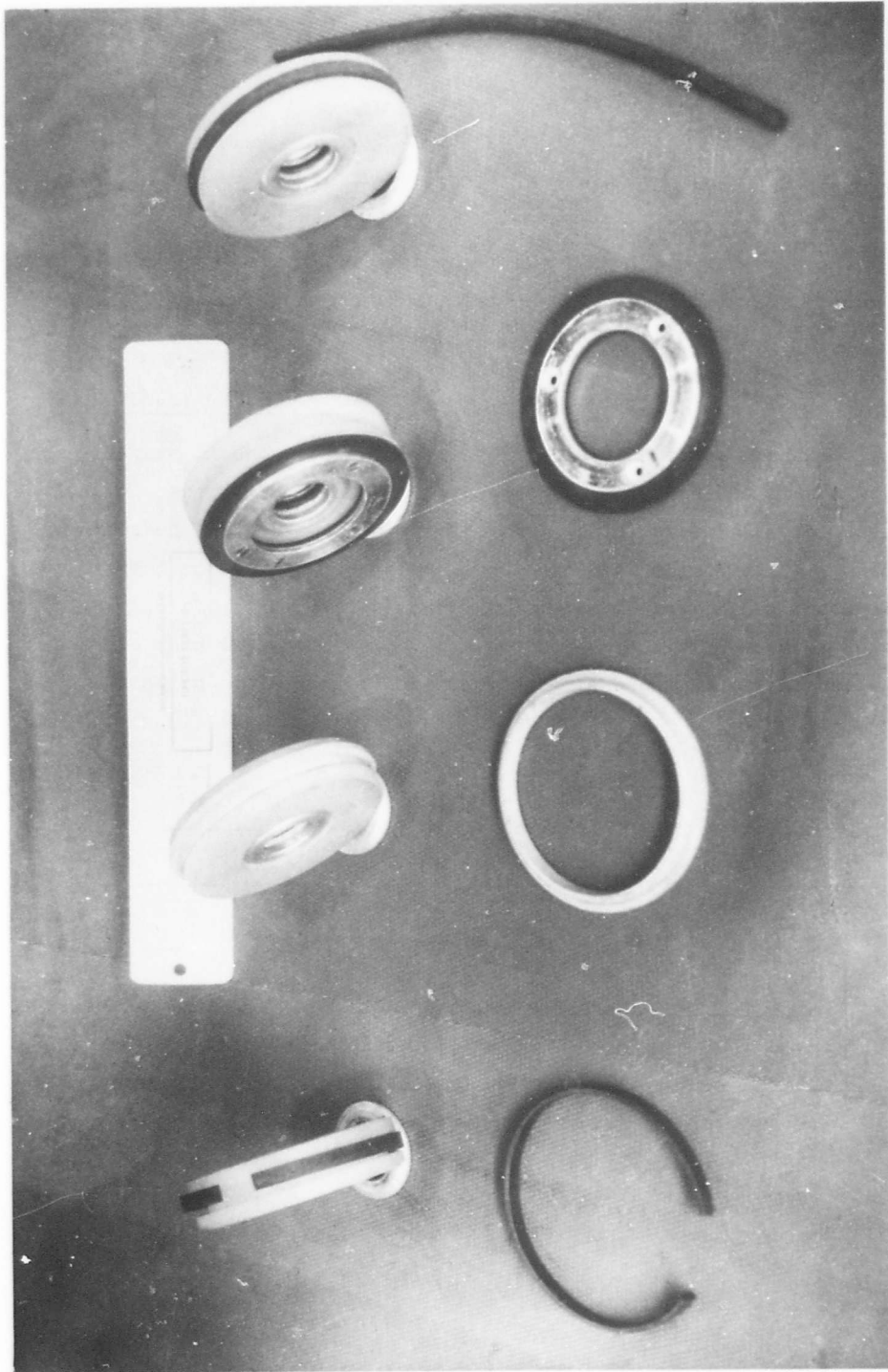


Fig. 9 - Four sealing rings, evaluated for low friction

which permitted studies of the dynamic properties of the VIM under pressure conditions. Results of these tests are tabulated below and charted on Figure 10 as Run #1.

<u>Data from Run #1</u>			
<u>Input Frequency</u>		<u>Output Amplitude</u>	<u>Transmissibility (%)</u>
<u>cps</u>	<u>rad./sec.</u>	<u>(inches)</u>	
1.67	10.5	.040	100
3.33	20.9	.050	100+ resonance
5.0	31.4	.050	100+ resonance
6.67	41.9	.055	100+ resonance
8.33	52.4	.033	82.5
10.0	62.8	.021	52.5
11.7	73.3	.014	35.0
13.3	83.7	.012	30.0
15.0	94.2	.010	25.0
16.7	104.7	.008	20.0

Test Conditions

3 Pistons - No Seals

Radial clearance .020 inch

Input amplitude .040 inch

Soft spring 10 lbs./foot

Hard spring (rubber) 750 lbs./foot

Water pressure 14.5 psi

Total force developed 30 lbs.

Attenuation readout by dial indicator

In an effort to improve the performance of the VIM, the three pistons were fitted with "O" rings. These rings were fabricated from soft 1/4-inch rubber tubing. An additional modification in the preceding test conditions was to vent the water input supply. This was accomplished by installing a hose extending 12 ft. vertically to match the water pressure of 6 psi. The force developed by the three pistons was 75 pounds. Results of this test follow and are plotted as Run #2 in Figure 10.

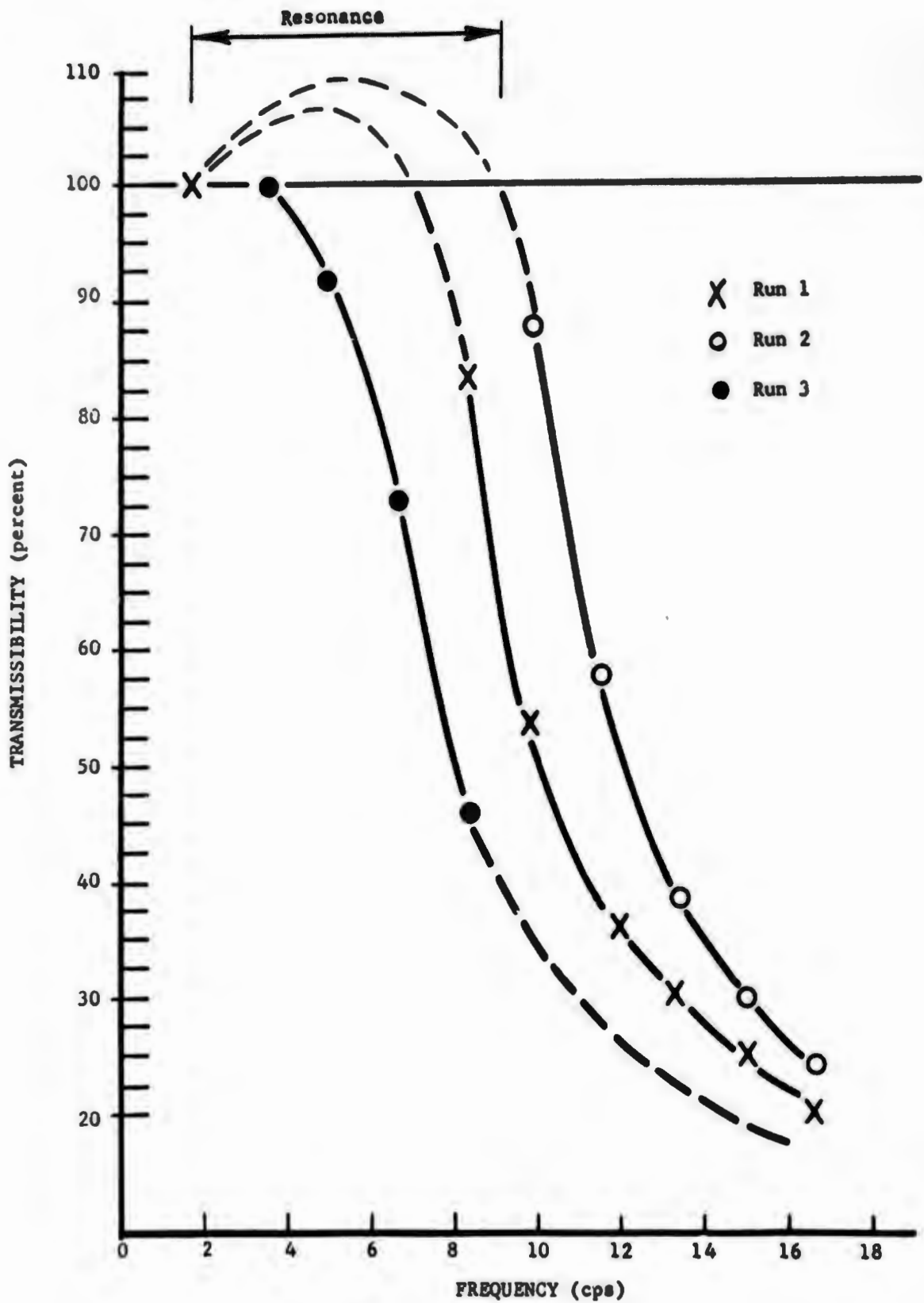


Fig.10 - Attenuating capacity of VIM  
(input amplitude = .040 inch)

Data from Run #2

<u>Input Frequency</u>		<u>Output Amplitude</u>	<u>Transmissibility</u>
<u>cps</u>	<u>rad./sec.</u>	<u>(inches)</u>	<u>(percent)</u>
1.67	10.5	.040	100
3.33	20.9	.045	100+ resonance
5.0	31.4	.045	100+ resonance
6.67	41.9	.070	100+ resonance
8.33	52.4	.055	100+ resonance
10.0	62.8	.035	88
11.7	73.3	.023	58
13.3	83.7	.015	38
15.0	94.2	.012	30
16.7	104.7	.009	23

Final trials were carried out after additional changes in the VIM configuration were made. Provision was made for feeding water into the piston zones in the reverse direction by means of a dip tube arrangement. The water flow was through the dip tube, into the piston tube aft end, back through the piston tube, into the various compartments, around the pistons, and out into the water trough through the front end scoop ports. The potentiometer-recorder system was used in this test (Run #3, Figure 10) to record the VIM output in a state of no load and no pressure. In this condition the VIM was submerged but not restrained, i.e., the grounding through the hard spring was eliminated. A manual sweep of the input from 1 cps to 15 cps resulted in a VIM output as shown in Figure 11. Except for a resonance zone between about 2 to 3 cps, the input and output were observed to be in phase. A shift in the zero point of oscillation may be observed on the chart. This was due to movement of the unrestrained VIM away from the input as the frequency was increased. This is attributed to unlike hydraulic properties of the physically different input and output sections. The net result was an imbalance in inertial forces associated with forward and reverse motion, with the forward force being of a higher value. To use an electrical analogue, the system tends to rectify.



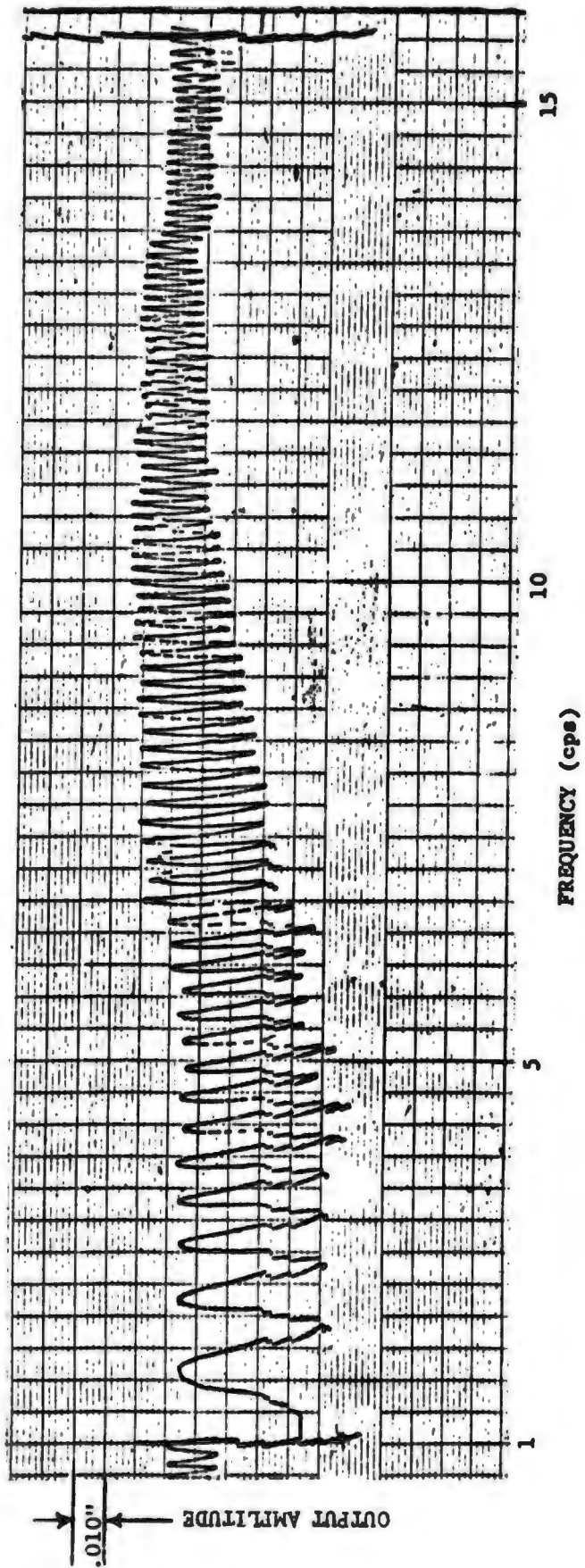


Fig. 11 - Output amplitude of VIM under no load as a function of frequency  
(Run #3 - water flow reversed)

## 6.0 DISCUSSION

If we plot the theoretical results and the experimental results together we obtain the curves given in Figure 12. It can readily be seen that the peak transmission is close to the peak at high frequency (associated with the total mass and the 1000 lb. spring). The height of this peak is much greater than in the calculation. This appears to be due to the friction force between the piston and cylinder, which leads to a very much larger value of  $C_1$ . Although there are no calculations allowing a direct comparison between the experimental and the theoretical data, the results obtained are consistent with this assumption.

In the Appendix we describe a design in which Bellofram bellows are suggested instead of pistons. Various practical considerations led us to abandon this design during the early part of the work. This decision might be reconsidered. The Bellofram would replace the dry or lubricated friction of the piston against the cylinder walls with the spring constant of the bellows. If this were small compared to the smaller spring constant an operable device might be obtained. Another possibility was suggested by Hugh Fitzpatrick of O.N.R. He proposed that the contact between the piston and the cylinder wall be made by a feather edge of rubber. This would substitute flexing the rubber for friction against the wall in the case of small displacements. Hence the spring constant of the thin rubber edge would be operative in the case of vibration. Only larger displacements associated with changes of speed would need to overcome the sliding friction. There are some difficulties in preventing the rubber edges from jamming but the possibilities of this design have by no means been studied in full.

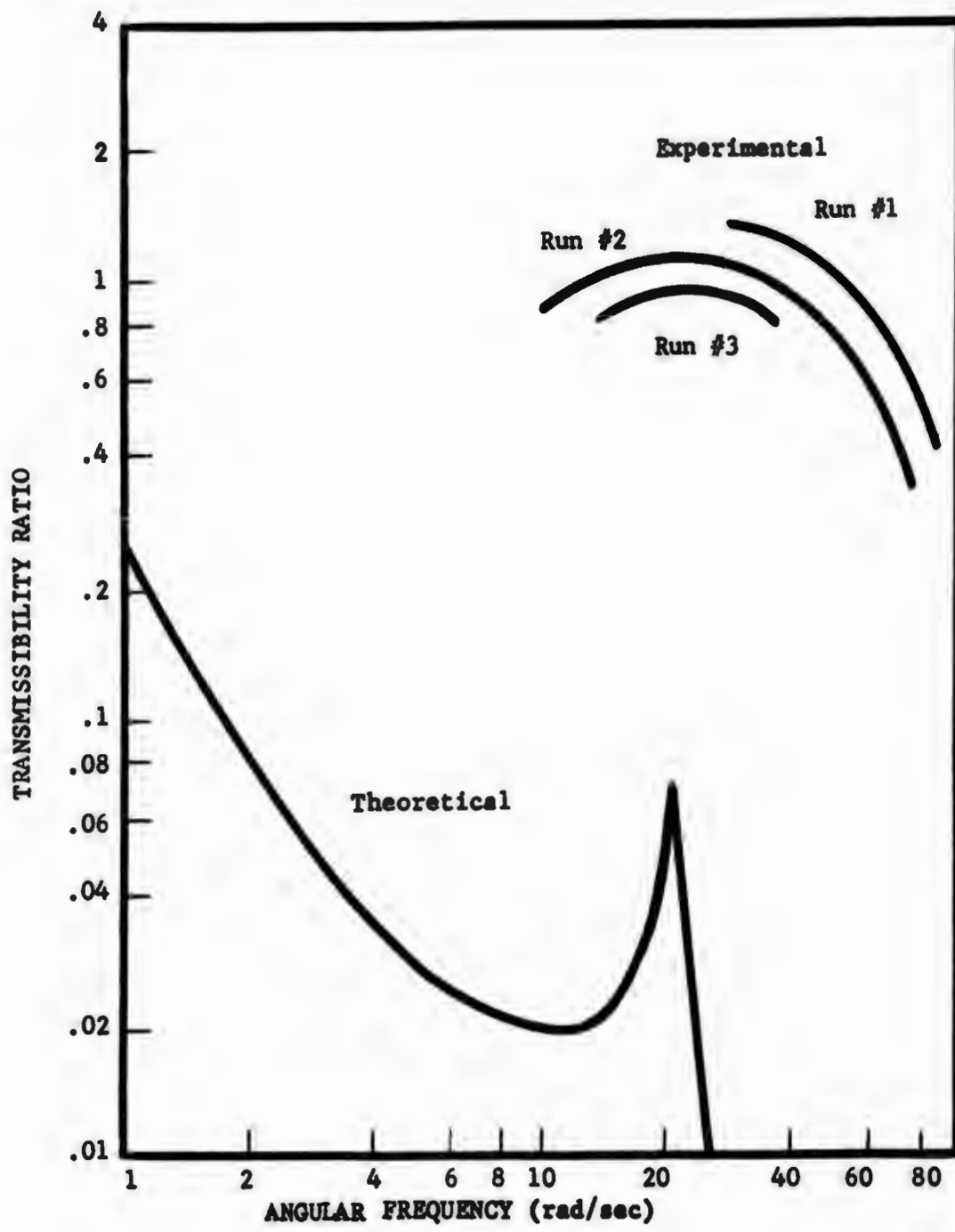


Fig. 12 - Comparison of theoretical and experimental results



## APPENDIX

### ALTERNATIVE VIM DESIGNS

The conceptual design of the VIM described in the body of this report was chosen over others because of its simplicity and reliability. To aid other investigators who might continue this work we are including brief descriptions of other designs considered and, for various reasons, rejected.

#### VIM - PULLEY AMPLIFICATION

Figure 1A shows a schematic representation of the first design considered. As shown, the dynamic pressure ( $p_D$ ) acts on the piston which in turn pushes against the rubber block #2. This force  $F$  ( $F = p_D \times \text{area of piston}$ ) puts the pulley line into tension of magnitude  $F$ . Consequently in the figure below there is a force  $2F$  pulling on block #3 which in turn is connected to the towed body. This gives us a force amplification of two and allows us to choose block #3 as the hard spring and block #2 as the soft spring.

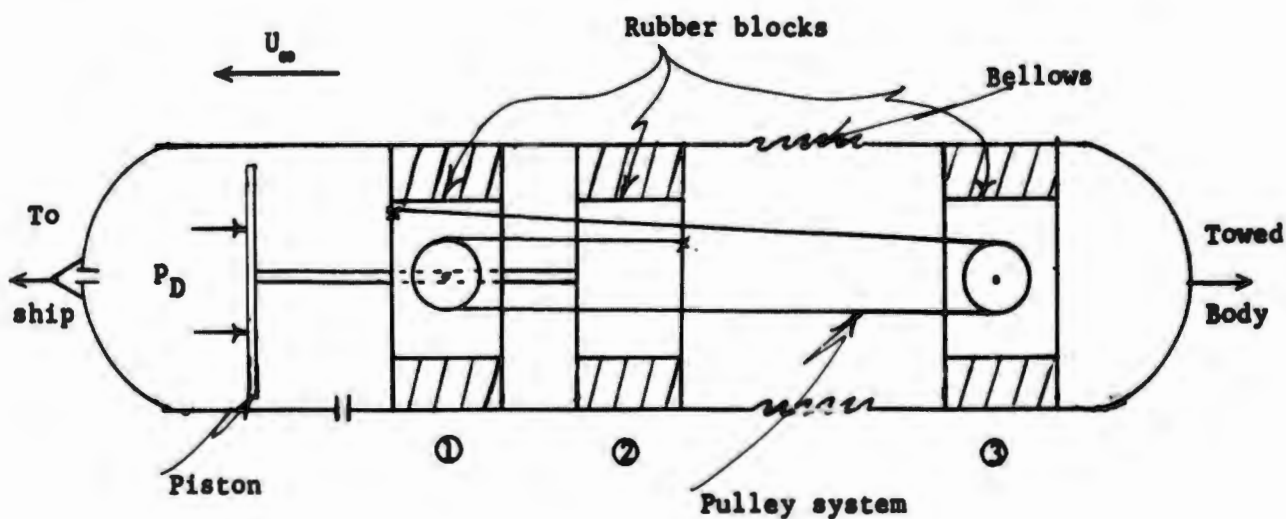


Fig. 1A - VIM - pulley amplification

For the system under consideration it is necessary to have an amplification factor of around eight. Although this could be achieved with a pulley system it would be quite clumsy and we feel unreliable. For this reason we chose to investigate hydraulic amplification systems and leave an analysis of the pulley system to investigators who might find a low amplification system suitable.

**VIM - HYDRAULIC AMPLIFICATION**

Figure 2A shows a schematic representation of a VIM which uses hydraulic amplification to increase the dynamic pressure. The VIM is shown traveling from right to left at a velocity  $U_\infty$ . The dynamic pressure acts on piston #2 and is amplified by piston #1 as shown. The resulting pressure  $p_2$  acts on piston #3. The force ( $p_2 \times$  the area of piston #3) equals the drag force and is transmitted through spring #1 to the casing. It is obvious that there need be no force acting on spring #1, and thus it can be chosen to have a small spring constant.

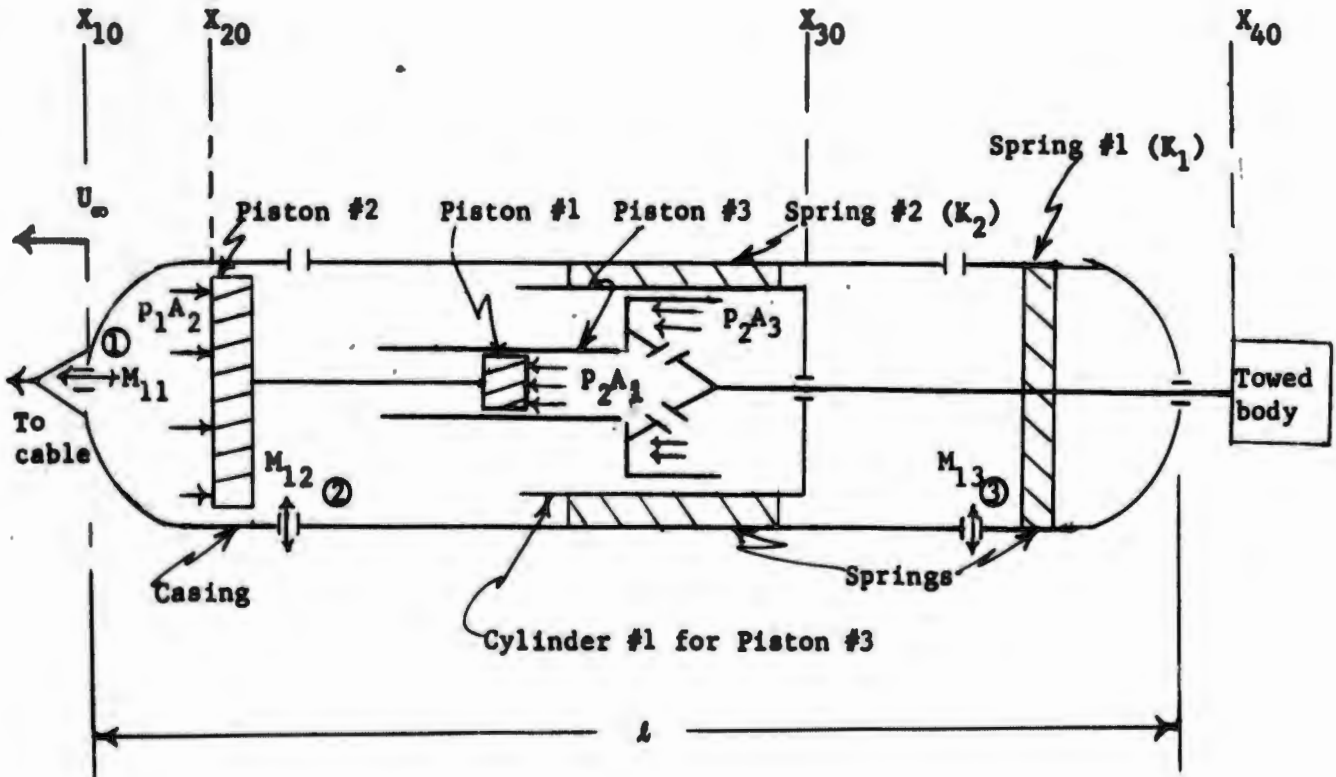


Fig. 2A - VIM - hydraulic amplification

High frequency disturbances will be damped out by spring #2. The behavior of the VIM at low frequencies is a much more complicated affair. It is necessary that when the casing of the VIM is subject to an acceleration, piston #2 move to the left with respect to the casing. This allows piston #3 to move right relative to the casing. The reverse is necessary when the VIM casing is decelerated. This behavior is required to make the transmissibility ratio less than one. This ratio is a measure of the attenuation of the system.

Analyzing this model in the same way as was done for the feasibility design we get for the transmissibility ratio:

$$|W(i\omega)| = \left| \frac{\frac{a_{13}a_{22}}{a_{23}^2} - \frac{a_{12}}{a_{23}}}{\frac{a_{22}a_{33}}{a_{23}^2} - 1} \right| \quad (1)$$

where:

- $a_{12} = (\alpha K_2' - \omega^2 M_{11}) + i\omega \alpha c_2$
- $a_{13} = (\beta K_2' + K_1') + i\omega(\beta c_2 + c_1)$
- $a_{22} = (\alpha^2 K_2' - \omega^2 \{M_2 + \alpha M_3 + M_{11}\}) + i\omega \alpha^2 c_2$
- $a_{23} = (\alpha \beta K_2' - \omega^2 \alpha \beta M_3) + i\omega \alpha \beta c_2$
- $a_{33} = (\beta^2 K_2' + K_1' - \omega^2 \beta^2 M_3 + M_4) + i\omega(\beta^2 c_2 + c_1)$
- $\alpha = \frac{1}{\gamma}; \quad \beta = \frac{\gamma-1}{\gamma}$
- $\gamma = A_1/A_2$  (hydraulic amplification)
- $M_{11}$  = added mass due to flow in opening #1
- $M_2$  = mass of pistons 1 + 2
- $M_3$  = mass of cylinder 1
- $M_4$  = mass of piston 3 + towed body

Table IA summarizes some of the numerical results obtained from Equation 1 for various values of the parameters shown.

TABLE IA

Test No.	$M_2$	$M_3$	$M_{11}$	$M_4$	$K_2$	$K_1$	$C_2$	$C_1$	Transmissibility Ratio (at frequency $\omega$ )						
	$\frac{\text{lb}_f\text{-sec}^2}{\text{ft}^2}$				$\frac{\text{lb}_f}{\text{ft}}$	$\frac{\text{lb}_f\text{-sec}}{\text{ft}}$			$\omega = .01$	$\omega = .05$	$\omega = .10$	$\omega = .50$	$\omega = 1.0$	$\omega = 5.0$	$\omega = 10.0$
1	.03	.03	.03	30	300	5	1.0	100	1.002	1.030	1.044	0.897	0.655	0.166	0.285
2	.03	.03	.03	30	500	5	1.0	100	1.002	1.030	1.044	0.897	0.655	0.166	0.103
3	.03	.03	.08	30	500	5	1.0	100	1.002	1.030	1.044	0.893	0.649	0.167	0.293
4	.03	.03	.03	30	500	20	1.0	100	1.001	1.014	1.049	1.651	0.717	0.166	0.103
5	.3	.15	.03	30	300	5	10.	500	1.001	1.002	1.002	0.994	0.969	0.790	0.407
6	.3	.15	.03	30	1000	10	10.	500	1.001	1.004	1.004	0.996	0.972	0.603	0.496

$\gamma = 7.2$  for all tests

Frequency in rad/sec

Although not conclusive, a comparison of tests #2 and #3 indicates that variations in the added mass  $M_{11}$ , at least in this limited range, do not affect the transmissibility ratio at low frequencies.

At high frequencies the mass  $M_{11}$  would be important if its magnitude were comparable to that of the other bodies, i.e., the mass of the VIM and the towed body. It is easy to show that this is not the case. For this reason we ignored its effect in the analysis given in the body of the report.

VIM - FLUID AMPLIFIER

Figure 3A shows a schematic representation of a VIM incorporating a fluid amplifier.



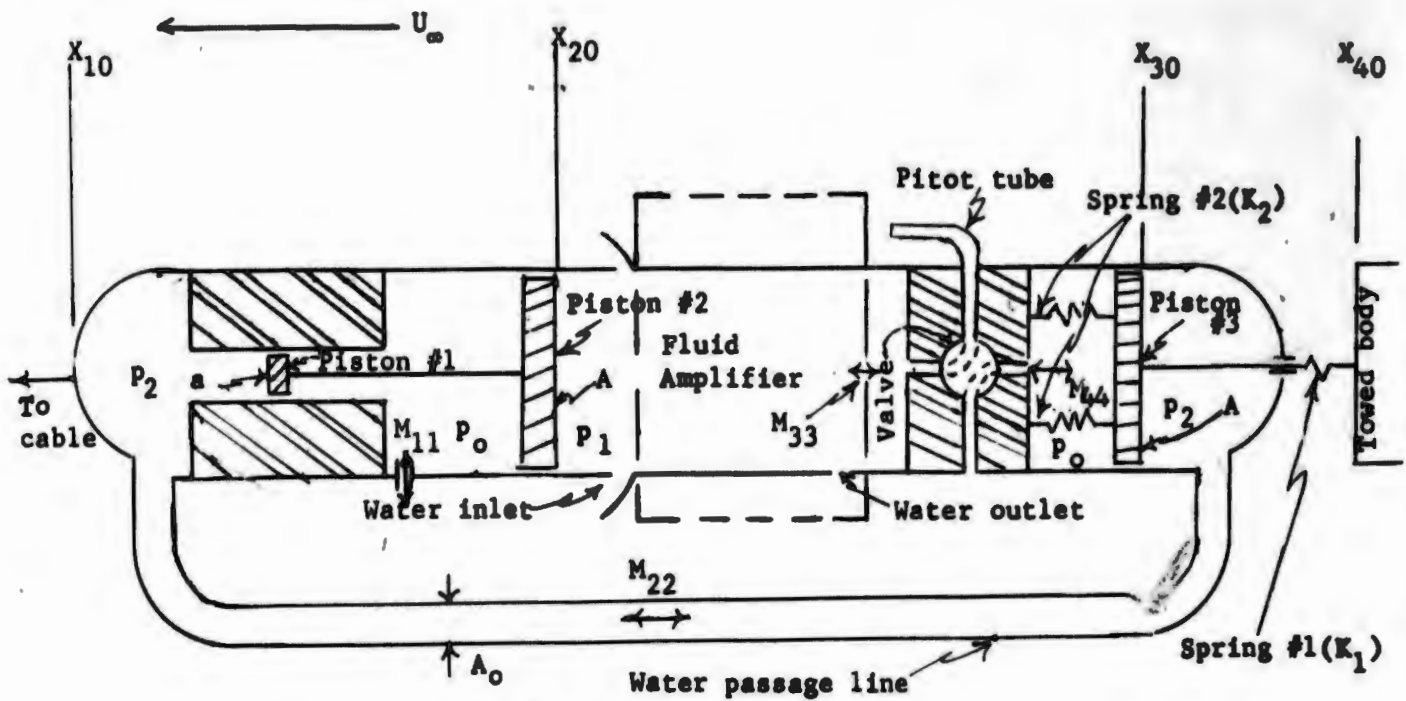


Fig. 3A - VIM - fluid amplification

This design uses the same principles as that in the previous one. That is, the drag force is balanced by the dynamic pressure so that there is no net force on the soft spring at equilibrium conditions. The only basic difference is the incorporation of an active element (in this case a fluid amplifier) to insure that the pistons in the VIM move in the proper direction to insure attenuation when the VIM is subject to an accelerating or decelerating force. The operating principles for this design is the same as for the previous one, the only difference being the inclusion of a fluid amplifier.

The fluid amplifier provides a method of switching the valve from the position shown to its opposite position when the VIM is accelerated. When this happens the pressure  $p_1$  acting on piston #2 decreases to  $p_0$  (the static pressure) and  $p_0$  which is acting on piston #3 increases to  $p_1$ . Pressure  $p_2$  consequently decreases proportionally to the change between  $p_0$  and  $p_1$ . When this happens piston #3, and consequently the towed body, moves to the right relative to the VIM, thereby extending

spring #2. This is a mass-spring-mass system capable of damping out low frequencies.

When the VIM is decelerated the fluid amplifier switches the valve back to the position shown. This allows piston #3 to move forward relative to the VIM thereby compressing the springs.

Figure 4A illustrates a fluid amplifier which could be used to switch the valve when necessary. It is called a Stream Interaction Amplifier. Its principle of operation is as follows:

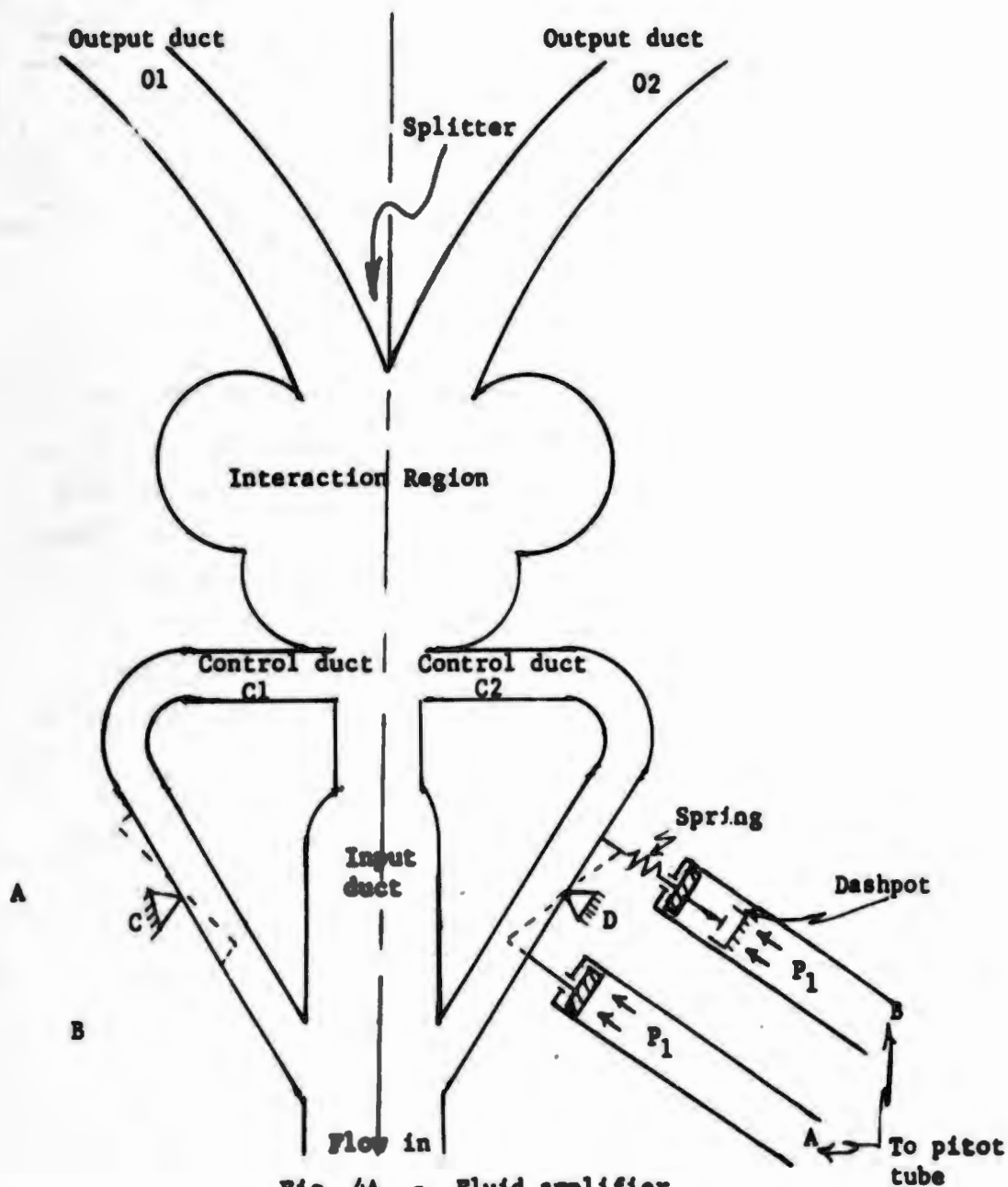


Fig. 4A - Fluid amplifier

The chamber is shaped to avoid the Coanda effect and the resulting power-flow attachment to the wall of an output duct. In the absence of a control flow, the flow strikes the splitter and divides evenly between the two output ducts. If a control flow is applied to duct C1 the power jet is deflected so that more of the power output flows through duct O2 and less flows through duct O1. Power jet deflection is proportional to the control flow, and depends on the momentum flux of the power jet and the control jet. If opposite control signals are applied simultaneously, power jet deflection varies in proportion to the differential control signal momentum flux.

By referring to Figure 4A it can be seen that under steady state conditions the flow through each control duct will be identical, therefore the power stream will be split in half. This power stream comes through the water inlet shown. Cylinders A & B are connected to a pitot tube not shown, therefore  $p_1 = \frac{1}{2} \rho U_{\infty}^2$ . If each half of the flow impinges on opposite sides of the valve shown in Figure 3A, no motion of the valve will occur. (Details of this have not been worked out yet.) To make sure that the valve is in the position shown when jets of equal force hit it, a spring can be put on the valve to apply a small force to keep it at the position shown.

If the VIM is suddenly accelerated,  $p_1$  in cylinders A & B begins to increase. (Refer now to the right side of Figure 4A.) When this happens the piston in A will move up while the piston in B lags behind because of the dashpot. Consequently the wall in control duct C2 can rotate about the pivot D, thereby decreasing the flow in C2. On the opposite side a stop prevents the wall in C1 from rotating about C, thereby not affecting the flow through C1. Due to this, there will now be a differential control flow and the output flow will increase in O2 and decrease in O1. Jets of different momentum will now be impinging on opposite sides of the valve thereby causing the valve to switch to its opposite position. This situation will be reversed when the VIM is decelerated. In this way, switching of the valve can be accomplished.

A study of fluid amplifiers has not been made, therefore the practicality of using them is not known by us at the present time. Because of the complexity of this design, work on it was deferred until the test results from the design described in the body of the report have been evaluated.

#### VIM - BELLOFRAM SYSTEM

Preliminary design work showed that a passive hydraulic force amplifier would not be practical. Problems with seals and alignment of internal components would have been very difficult to solve. Therefore, it was decided to obtain the balancing force directly by adding more primary pistons which are exposed to the dynamic pressure. This was also done for the feasibility design. This force is then transmitted to a separate hydraulic system which in turn transmits the balancing force to the soft spring, effectively nullifying the drag force on that spring. Figure 6A gives a representation of this system.

The value of this system over the hydraulic systems described is that:

- (1) seals on the primary pistons are not critical and
- (2) a working system using Belloframs insures a zero leakage seal.

A preliminary design was worked out for the Bellofram system and the minimum length (excluding flotation equipment) was calculated. This is plotted as a function of diameter in Figure 5A. The operating system would be 10 feet long (minimum) with a 3 inch diameter. This length could be cut to 7-1/2 feet if the diameter were 4 inches.

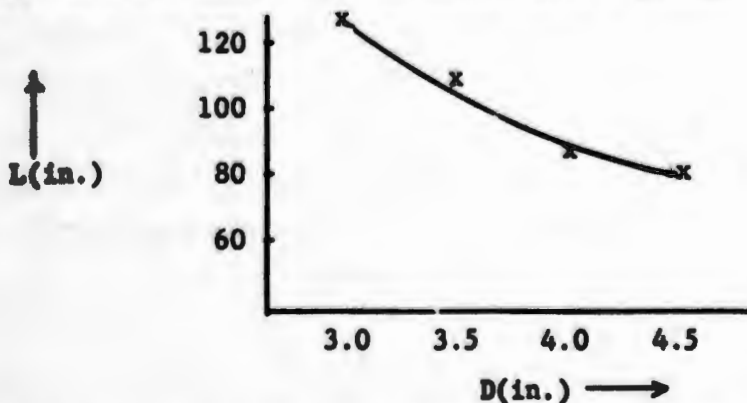
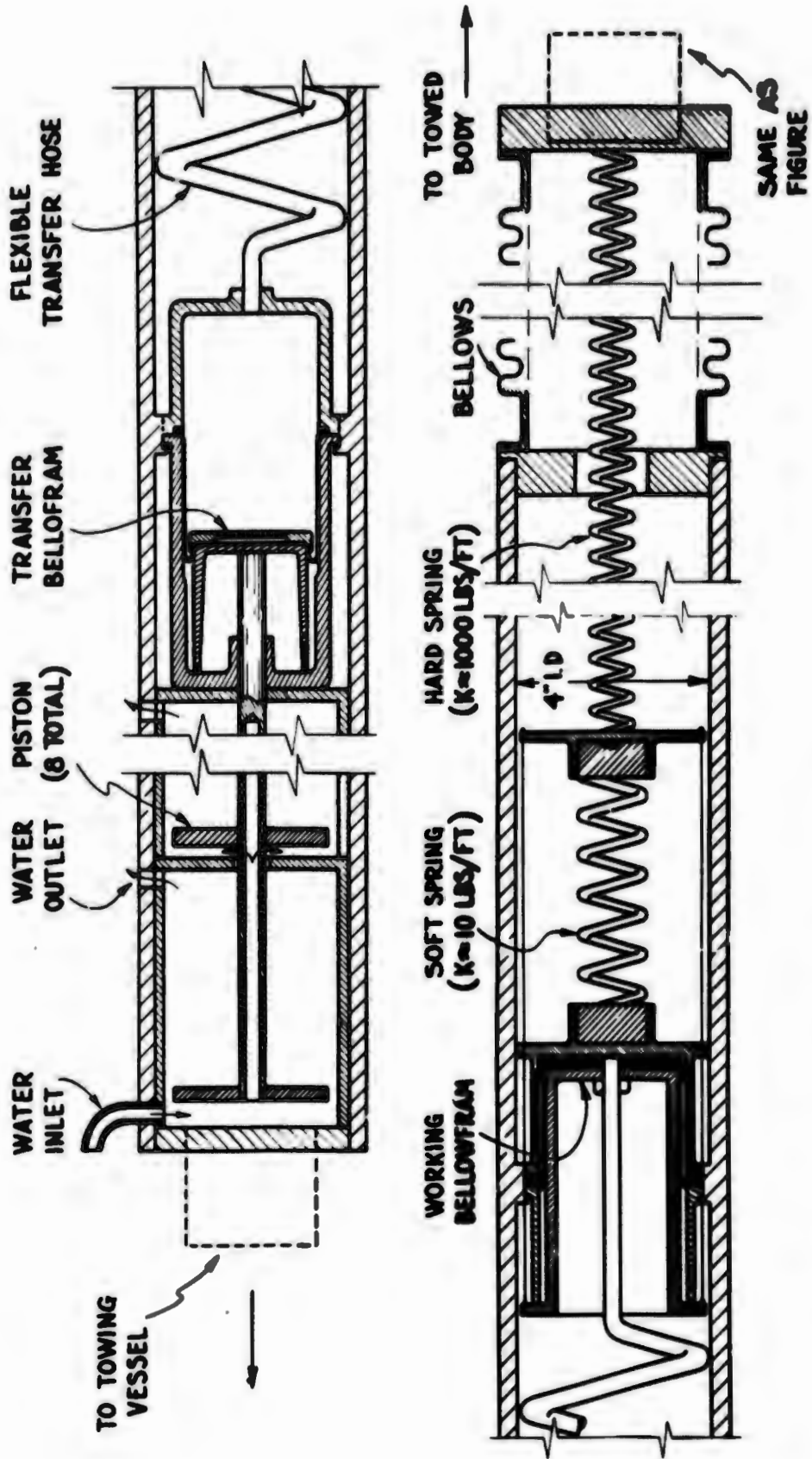


Fig. 5A - Length vs. diameter for Bellofram VIM



**NOTE / VIM SHOWN MINUS BUOYANCY CONTAINERS**

**Fig. 6A - VIM - Bellofram system**

Since the contribution of the VIM to the total drag of the system is small there is no reason why its diameter cannot be 1-1/2 inches larger, provided that its ends are properly faired to avoid the generation of unnecessary hydrodynamic noise. We therefore chose for this design and for the feasibility design an inside diameter of 4 inches which would result in an outside diameter of about 4-1/2 inches.

The final length of the VIM depends upon the amount of flotation required. In an aluminum or glass filament structure the containers required for neutral buoyancy would have doubled its length. There are other materials, however, which are much lighter, yet strong enough to support the wall loads in the casing. One of these is polypropylene, which has a density of .91 and is also impervious to sea water. This could reduce the length of the buoyancy section needed to a foot or so. This material is recommended for the first model.

The Bellofram design was the first one to be considered during the growth of this project. It was superseded by the design actually used because the Bellofram design is more difficult to assemble, more complex, and, because of its complexity, less reliable. It is important to keep in mind that, in principle, these two designs are equivalent. If one of them should show itself to be fundamentally unsound then neither of them can be expected to work. In this event, attention should be focused on the VIM with the fluid amplifier or on a possible design mentioned in the next section. However, in view of the nature of the difficulties met with the array of pistons, the Bellofram design might be reconsidered.

#### VIM - PUMP SYSTEM

The possibility of using a pump to amplify the pressure, as opposed to using a bank of pistons, was briefly considered but not carefully investigated.



## DOCUMENT CONTROL DATA - R &amp; D

(Security classification of title, body of abstract and indexing annotation must be entered when the overall report is classified)

1. ORIGINATING ACTIVITY (Corporate author) United States Rubber Company (now Uniroyal, Inc.) Research Center Wayne, New Jersey 07470		2a. REPORT SECURITY CLASSIFICATION <b>UNCLASSIFIED</b>	
		2b. GROUP	
3. REPORT TITLE  Design, Construction and Testing of a Vibration Isolation Module			
4. DESCRIPTIVE NOTES (Type of report and, inclusive dates) Final Report			
5. AUTHOR(S) (First name, middle initial, last name)  James J. Neville, Fitzhugh W. Boggs, and John Thompsen			
6. REPORT DATE February 1969	7a. TOTAL NO. OF PAGES 53	7b. NO. OF REFS 1	
8a. CONTRACT OR GRANT NO. Contract No. Nonr-4947(00)	9a. ORIGINATOR'S REPORT NUMBER(S)		
b. PROJECT NO.			
c.	9b. OTHER REPORT NO(S) (Any other numbers that may be assigned this report)		
d.			
10. DISTRIBUTION STATEMENT			
11. SUPPLEMENTARY NOTES  //		12. SPONSORING MILITARY ACTIVITY Office of Naval Research Department of the Navy	
13. ABSTRACT A conceptual design for a Vibration Isolation Module (VIM) is described and analyzed. The VIM was designed to attenuate significantly vibrations over a frequency range from $10^{-1}$ cps to higher frequencies likely to be encountered. A prototype VIM was constructed and tested. It involved the use of a multiple piston arrangement in which the stagnation pressure at the fore end of the VIM was converted to a force which matched the drag of the towed body. In this way it was possible to preserve a low modulus while avoiding a high elongation, since the main towing effort was balanced in such a way that the damping mechanism carried only the fluctuation and not the active force. During tests, the VIM did not attenuate in the frequency range for which it was designed (below 5 cycles per second). The primary cause of the failure to meet design requirements was the high level of the frictional forces. Detrimental hydrodynamic forces were also encountered.			

14. KEY WORDS	LINK A		LINK B		LINK C	
	ROLE	WT	ROLE	WT	ROLE	WT
Isolation Module						
Vibration Isolation						
Hydroelastic Stability						